KYUSHU UNIVERSITY

Measurement of cross sections in Higgs boson decays to four leptons with the ATLAS detector

Susumu Oda

Kyushu University (Japan)

On behalf the ATLAS Collaboration

The European Physical Society Conference on High Energy Physics (EPS-HEP)

2019-07-11, Ghent, Belgium

ATLAS EXPERIMENT

EUROPEAN PHYSICAL SOCIETY HEP2019

Introduction

- Higgs boson decays to four leptons can be selected with a very high purity and are very well suited for measurements of Higgs boson properties, despite the small $H \to ZZ^* \to 4\ell$ branching ratio.

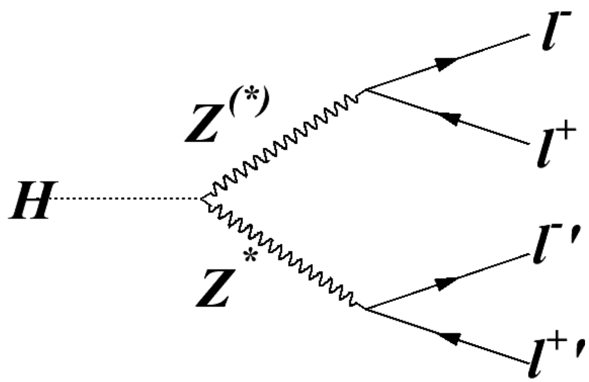

Production process		σ [pb]
ggF	$(gg \to H)$	48.6 ± 2.4
VBF	$(qq' \to Hqq')$	3.78 ± 0.08
WH	$(q\bar{q}' \to WH)$	1.373 ± 0.028
ZH	$(q\bar{q}/gg \to ZH)$	0.88 ± 0.04
ttH	$(q\bar{q}/gg \to t\bar{t}H)$	0.51 ± 0.05
bbH	$(q\bar{q}/gg \to b\bar{b}H)$	0.49 ± 0.12
tH	$(q\bar{q}/gg \to tH)$	0.09 ± 0.01
Decay process		$\mathcal{B}\ [\cdot 10^{-4}]$
$H \to ZZ^*$		262 ± 6
$H \to ZZ^* \to 4\ell$		1.240 ± 0.027

For $m_H = 125$ GeV

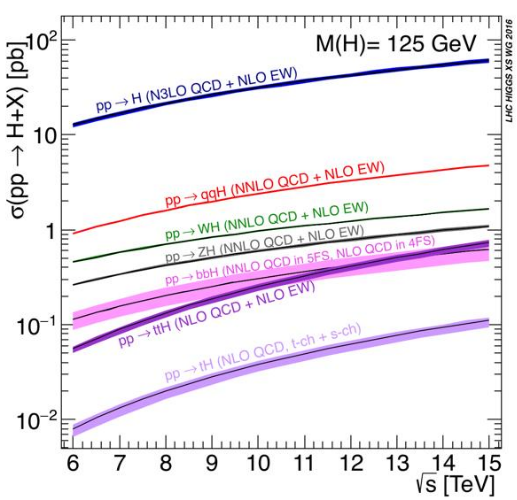

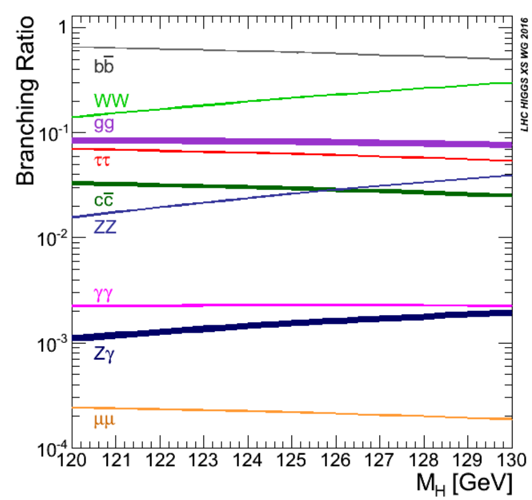

Main updates from previous results

- Previous 13 TeV results
  - JHEP 10 (2017) 132 (36.1 fb^{-1})
  - JHEP 03 (2018) 095 (36.1 fb^{-1})
  - ATLAS-CONF-2018-018 (79.8 fb^{-1})
- New results
  - **ATLAS-CONF-2019-025** (139 fb^{-1})

1. Use the full Run 2 statistics (2015—2018)
2. Improved lepton isolation to mitigate the impact of pileup
3. Constraint of the major non-resonant ZZ^* background from dedicated data sidebands
4. Unfolding method exploiting the full response matrix
5. Additional reconstructed event categories and new discriminants to enhance the sensitivity to the various production modes
6. Dedicated control region to constraint the tXX background

Cross section measurements

- Inclusive fiducial cross section
- Total cross section
- Differential fiducial cross section
  - $p_T^{4\ell}$ and N_{jets} : to test the SM prediction and constraint BSM effects because they are sensitive to
    - Higher-order QCD calculations
    - The modelling of gluon emission
    - The fractions of the different production modes
    - The Lagrangian structure of the Higgs boson interactions
- Production mode cross section
  - Simplified Template Cross Sections (STXS) framework

- To be model independent
  - Fiducial selection follows closely reconstruction-level selection.
  - Unfolding to correct for detector resolution and efficiency effects
    - Use likelihood fit including detector response matrix for unfolding
- Template fit of $m_{4\ell}$ distribution to extract the number of signal events

Event selection

- Signal mass window: $115 < m_{4\ell} < 130$ GeV
- SFOS: same-flavor opposite sign
- ME: matrix element for extra lepton(s) (VH-Lep, ttH-Lep) to avoid mispairing.

↓ Definition of the fiducial space

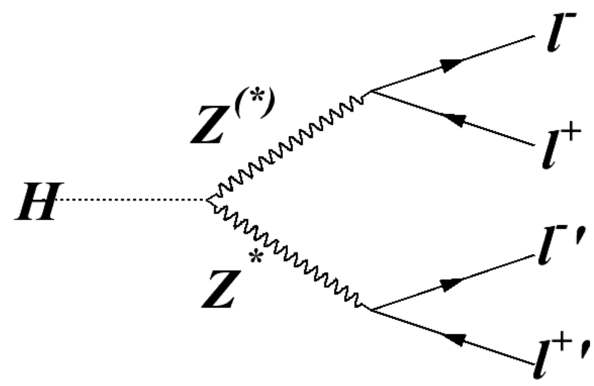

Leptons and jets	
Leptons	$p_T > 5$ GeV, $\lvert\eta\rvert < 2.7$
Jets	$p_T > 30$ GeV, $\lvert y\rvert < 4.4$
remove jets with	$\Delta R(\text{jet}, \ell) < 0.1$
Lepton selection and pairing	
Lepton kinematics	$p_T > 20, 15, 10$ GeV
Leading pair (m_{12})	SFOS lepton pair with smallest $\lvert m_Z - m_{\ell\ell}\rvert$
Subleading pair (m_{34})	remaining SFOS lepton pair with smallest $\lvert m_Z - m_{\ell\ell}\rvert$
Event selection (at most one quadruplet per event)	
Mass requirements	50 GeV$< m_{12} < 106$ GeV and 12 GeV $< m_{34} < 115$ GeV
Lepton separation	$\Delta R(\ell_i, \ell_j) > 0.1$
J/ψ veto	$m(\ell_i, \ell_j) > 5$ GeV for all SFOS lepton pairs
Mass window	105 GeV $< m_{4\ell} < 160$ GeV
If extra leptons with $p_T > 12$ GeV	Quadruplet with the largest ME

Response matrices for unfolding

- $N_i(m_{4\ell}) = \sum_j r_{ij} \cdot \left(1 + f_i^{\text{nonfid}}\right) \cdot \sigma_j^{\text{fid}} \cdot P(m_{4\ell}) \cdot \mathcal{L} + N_i^{\text{bkg}}(m_{4\ell})$
- $\sigma_j^{\text{fid}} = \sigma_j \cdot A_j \cdot \mathcal{B}(H \to ZZ^* \to 4\ell)$
- r_{ij} allows to correct for bin migrations and detector efficiencies.

↓ Unfolding for the differential measurements

$p_T^{4\ell}$

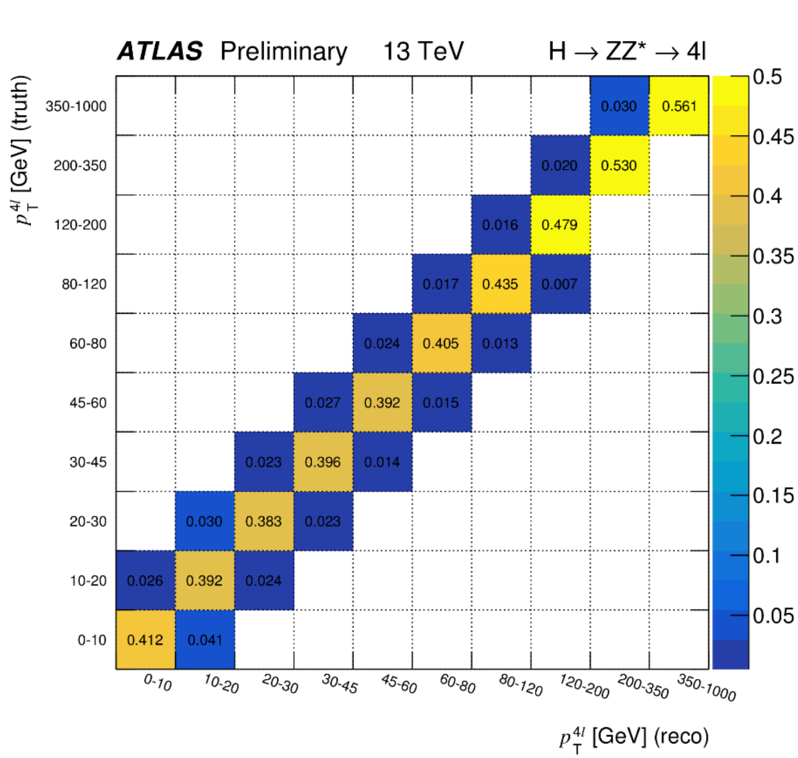

N_{jets}

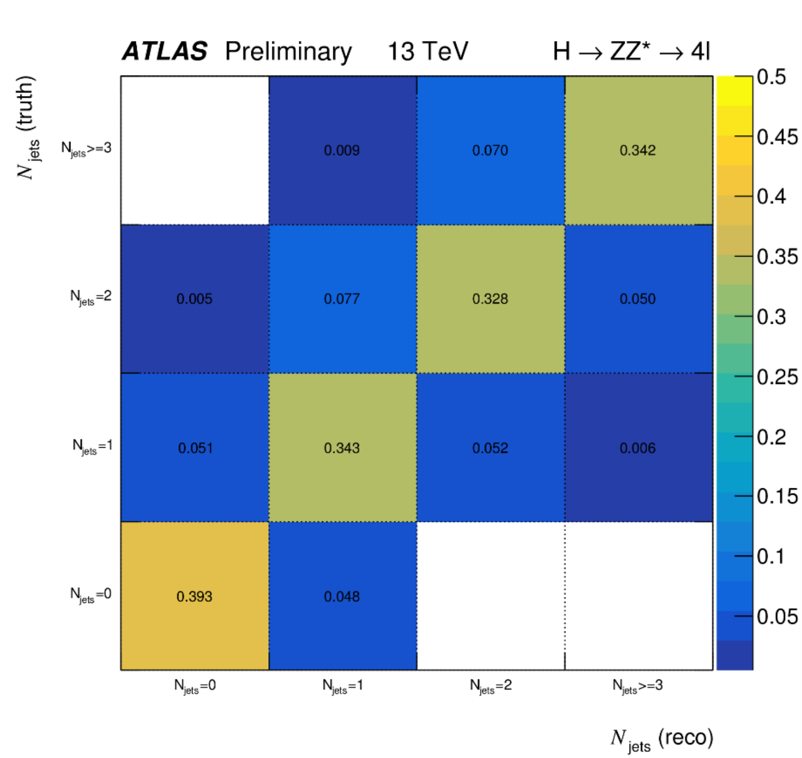

Simplified Template Cross Sections (STXS)

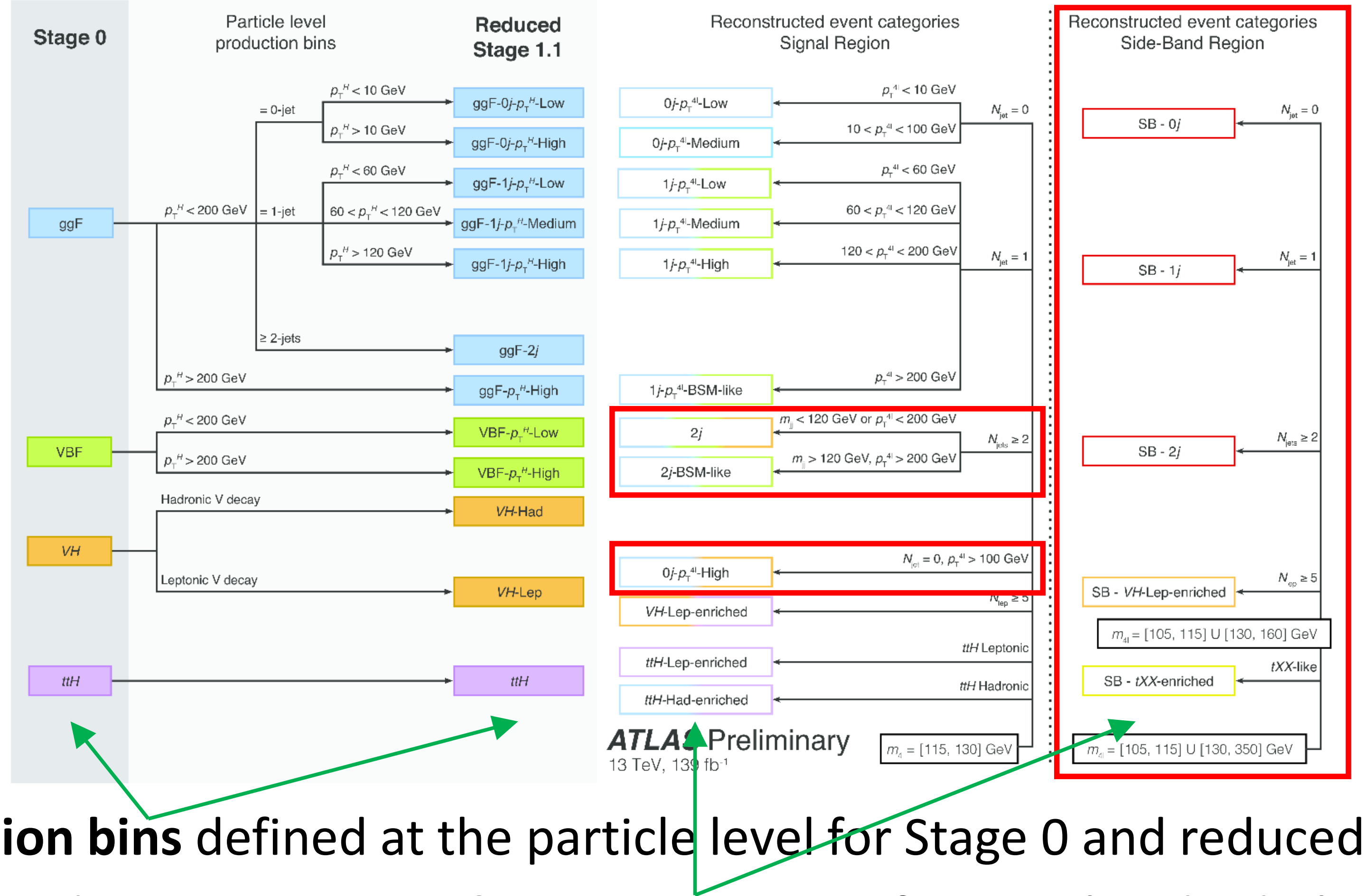

- **Production bins** defined at the particle level for Stage 0 and reduced Stage 1.1
- Corresponding **reconstructed event categories** for signal and side-bands
  - $2j$ category now consists of a BSM category and a $2j$ category (the rest) where neural network discriminants are used to separate VBF, ggF and VH-had.
  - New $0j$-$p_T^{4\ell}$-High category for VH with $Z \to \nu\nu$, or $W \to \ell\nu$ where ℓ is missing.
  - New side-band categories for backgrounds. ($105 - 115$ GeV and $130 - 350$ GeV)

SM signal composition (red. Stage 1.1)

- In terms of the reduced Stage 1.1 production bins in each reconstructed event category.
- The bbH contributions are included in the ggF production bins.
- To improve the sensitivity neural network discriminants are exploited.

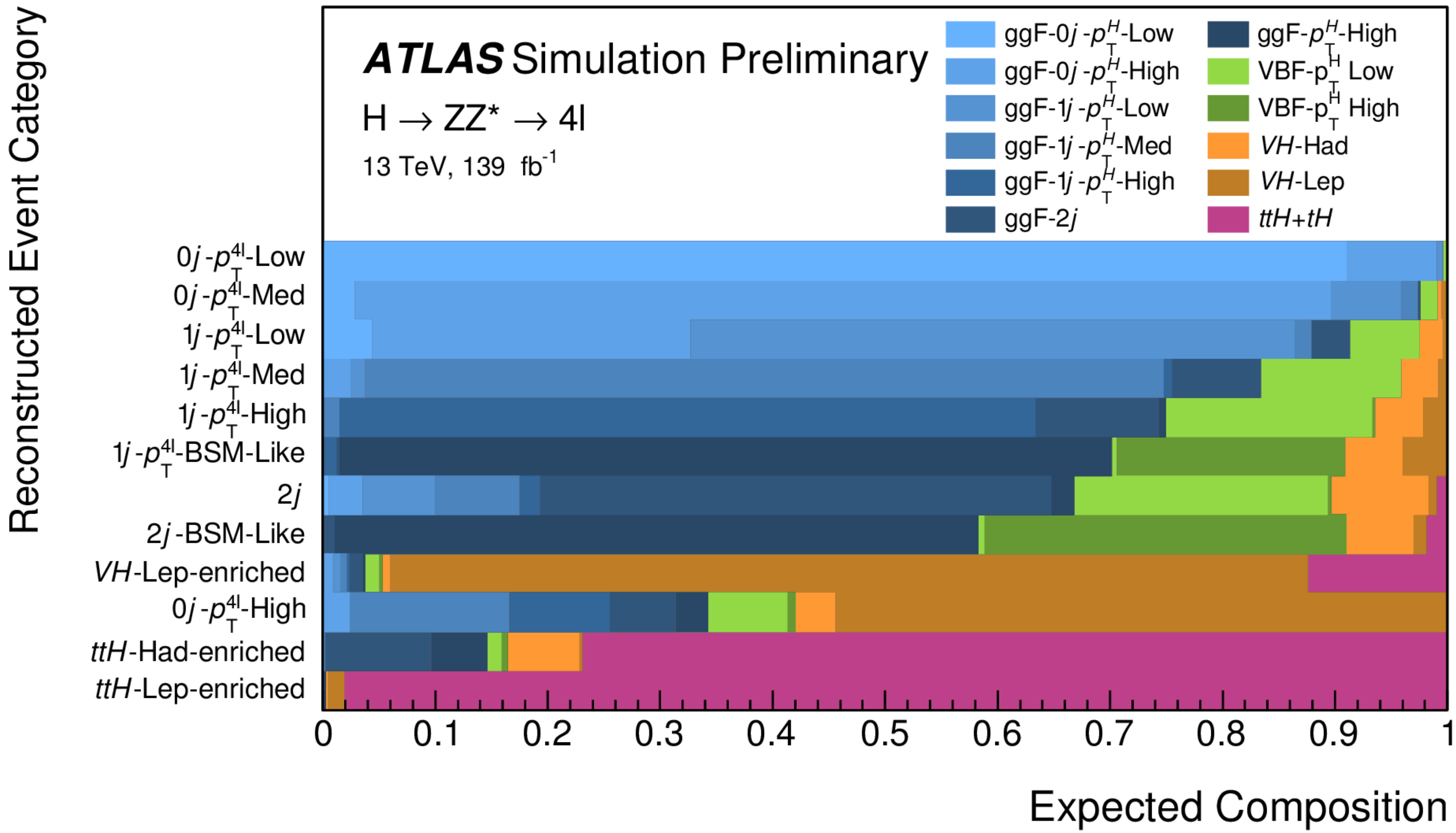

Neural network (NN) inputs

Category	Processes	MLP	Lep rNN	Jet rNN
$0j$	ggF,ZZ	$p_{\mathrm{T}}^{4\ell}$, D_{ZZ^*}, m_{12}, m_{34}, $\cos\theta^*$, $\cos\theta_1$, ϕ_{ZZ}	$p_{\mathrm{T},\ell}$, η_ℓ	n/a
$1j$-$p_{\mathrm{T}}^{4\ell}$-Low	ggF,VBF,ZZ	$p_{\mathrm{T}}^{4\ell}$, $p_{\mathrm{T},j}$, η_j, $\Delta R_{4\ell j}$, D_{ZZ^*}	$p_{\mathrm{T},\ell}$, η_ℓ	n/a
$1j$-$p_{\mathrm{T}}^{4\ell}$-Med	ggF, VBF, ZZ	$p_{\mathrm{T}}^{4\ell}$, $p_{\mathrm{T},j}$, η_j, $E_{\mathrm{T}}^{\mathrm{miss}}$, $\Delta R_{4\ell j}$, D_{ZZ^*}, $\eta_{4\ell}$	-	n/a
$1j$-$p_{\mathrm{T}}^{4\ell}$-High	ggF, VBF	$p_{\mathrm{T}}^{4\ell}$, $p_{\mathrm{T},j}$, η_j, $\Delta R_{4\ell j}$, $\eta_{4\ell}$, $E_{\mathrm{T}}^{\mathrm{miss}}$	$p_{\mathrm{T},\ell}$	n/a
$2j$	ggF, VBF, VH	m_{jj}, $\Delta\eta_{\mathrm{jj}}$, $p_{\mathrm{T},4\ell jj}$	$p_{\mathrm{T},\ell}$, η_ℓ	$p_{\mathrm{T},j}$, η_j
$2j$-BSM-like	ggF, VBF	$\Delta\eta_{\mathrm{jj}}$, $\Delta\eta_{4\ell jj}$, $p_{\mathrm{T},4\ell jj}$	$p_{\mathrm{T},\ell}$, η_ℓ	$p_{\mathrm{T},j}$, η_j
VH-Lep-enriched	ttH, VH	N_{jets}, $N_{b-\mathrm{jets}}$, $E_{\mathrm{T}}^{\mathrm{miss}}$, HT, $\ln(\lvert\mathcal{M}_{sig}\rvert^2)$	$p_{\mathrm{T},\ell}$	n/a
ttH-Had-enriched	ttH, tXX, ggF	$p_{\mathrm{T}}^{4\ell}$, m_{jj}, $\Delta\eta_{\mathrm{jj}}$, $p_{\mathrm{T},jj}$, $\min(\Delta R_{Zj})$, $\Delta\eta_{4\ell jj}$, N_{jets}, $N_{b-\mathrm{jets}}$, $E_{\mathrm{T}}^{\mathrm{miss}}$, $\min(\Delta R_{4\ell j})$, HT, $\ln(\lvert\mathcal{M}_{sig}\rvert^2)$	$p_{\mathrm{T},\ell}$, η_ℓ	$p_{\mathrm{T},j}$, η_j

- An improved performance was found with a structured neural network (multilayer perceptron, MLP) with inputs of
  - a recurrent NN (rNN) for the vectors of (p_T, η) for four leptons
  - another rNN for up to three jets
  - and another MLP with additional variables.
- The NN can separate 2 or 3 processes.
  - For an NN with 3-outputs (PDFs), a cut is applied to one output, using this output as a discriminant for the events passing the cut.
  - One of the other two outputs is used as a discriminant with the remained events.

Systematic uncertainties (Stage 0)

Measurement	Experimental uncertainties [%] Lum.	e, μ, pile-up	Jets, flavour tagging	Reducible backgr.	Theory uncertainties [%] ZZ^* backgr	tXX backgr.	PDF	Signal QCD scale	Signal Parton Shower	Composition
Fiducial cross section										
σ_{comb}	1.7	2.5	–	< 0.5	1	< 0.5	< 0.5	2	1	< 0.5
Per decay final state fiducial cross sections										
4μ	1.7	2.5	–	0.5	1	< 0.5	< 0.5	2	1	< 0.5
$4e$	1.7	7	–	0.5	1.5	< 0.5	< 0.5	2	0.5	< 0.5
$2\mu 2e$	1.7	5.5	–	0.5	1	< 0.5	< 0.5	2	1.5	< 0.5
$2e2\mu$	1.7	2.0	–	0.5	1	< 0.5	< 0.5	2	1	< 0.5
Stage-0 production bin cross sections										
ggF	1.7	1.5	1	0.5	1.5	< 0.5	0.5	1	2	–
VBF	1.7	1	4.5	0.5	2	0.5	1.5	8	6	–
VH	1.8	1.5	3.5	1	5	0.5	2	12	8	–
ttH	1.7	1	4.5	1	1	0.5	0.5	8	4	–

Many of systematic uncertainties have decreased.

- Luminosity
  - 2.8% → 1.7%
- Electron/muon reconstruction and identification efficiency and pileup dep.
  - Dominant
  - Reduced to about 50% of previous results
- Jet energy scale/resolution and b-tagging efficiencies
- Reducible background
- ZZ^* background
  - Reduced to about 60% of previous results
- tXX background
- Parton distribution functions
- QCD scales
- Showering algorithm
- Correction factor due to relative contribution of each production

Invariant mass and numbers of events

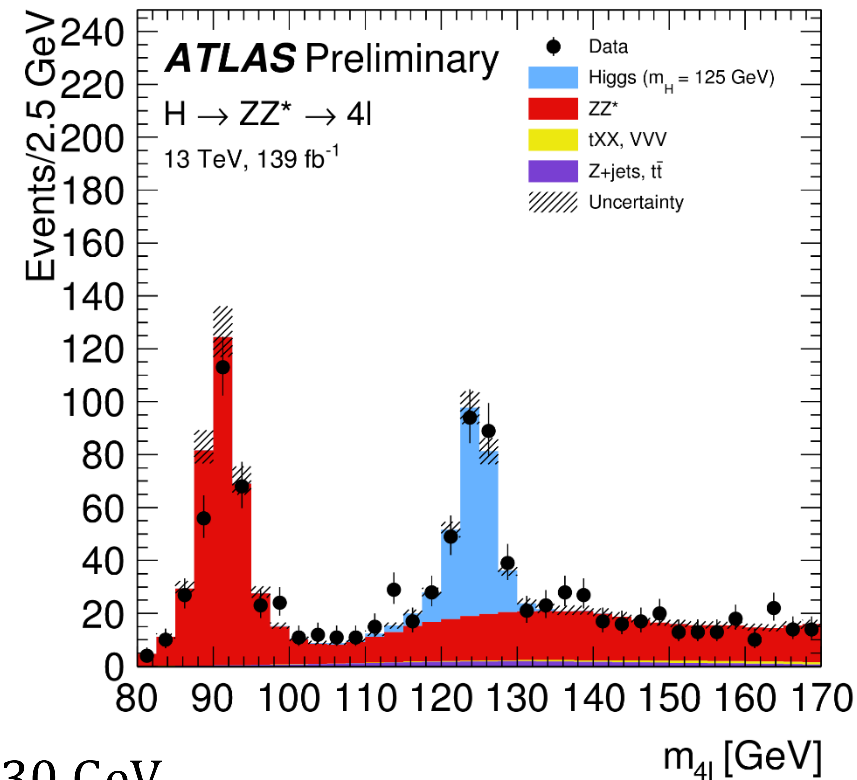

This distribution is pre-fit.

$115 \text{ GeV} < m_{4\ell} < 130 \text{ GeV}$

Final state	Signal	ZZ^* background	Other backgrounds	Total expected	Observed
4μ	78 ± 5	38.1 ± 2.2	2.87 ± 0.18	119 ± 5	118
$2e2\mu$	52.8 ± 3.1	26.1 ± 1.4	3.01 ± 0.19	81.9 ± 3.4	98
$2\mu2e$	40.0 ± 2.9	17.4 ± 1.3	3.5 ± 0.5	60.9 ± 3.2	57
$4e$	35.3 ± 2.6	15.1 ± 1.5	2.9 ± 0.4	53.3 ± 3.1	43
Total	206 ± 13	97 ± 6	12.3 ± 0.9	315 ± 14	316

Invariant mass distributions

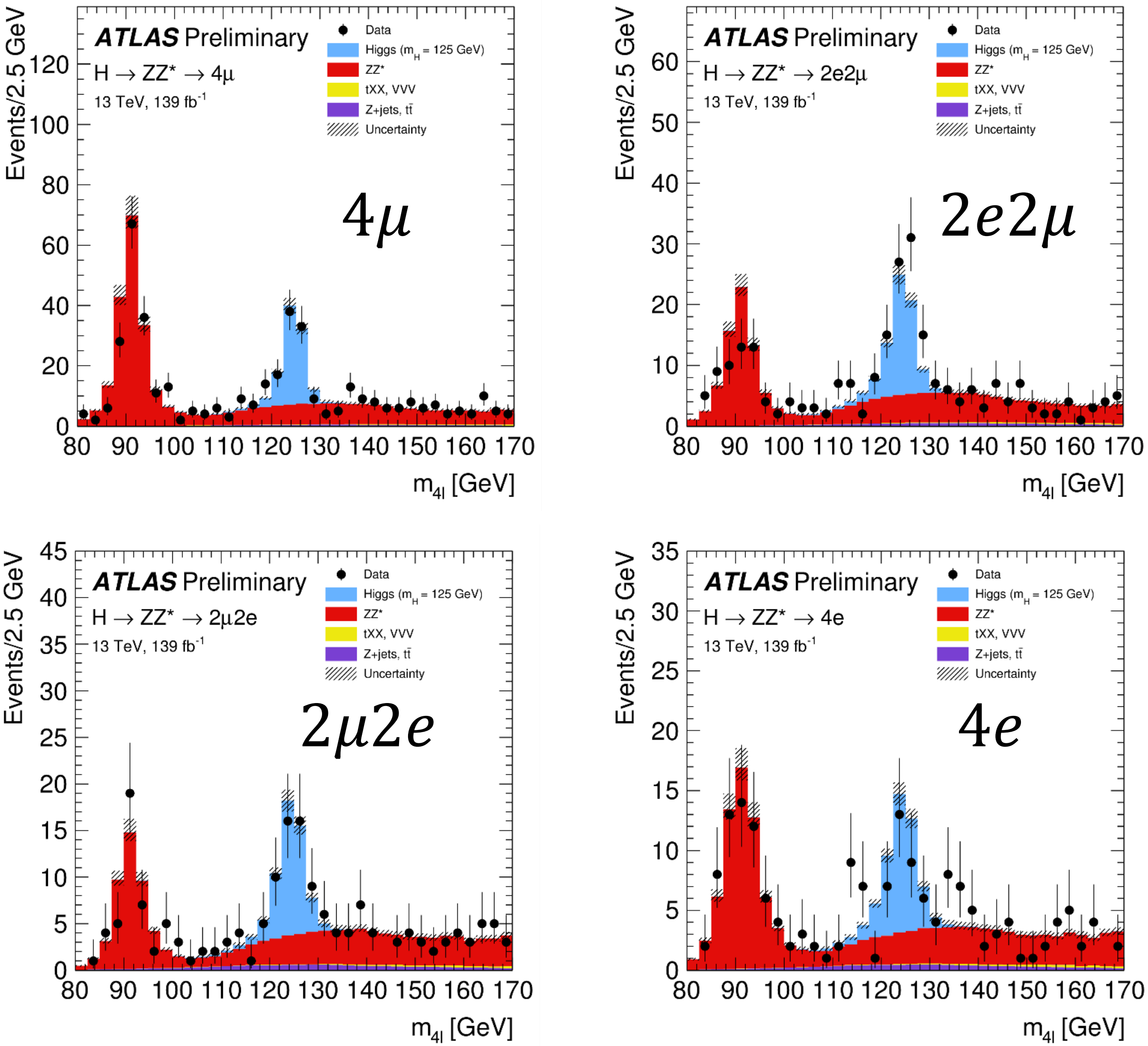

These distributions are pre-fit.

$p_T^{4\ell}$ and N_{jets}

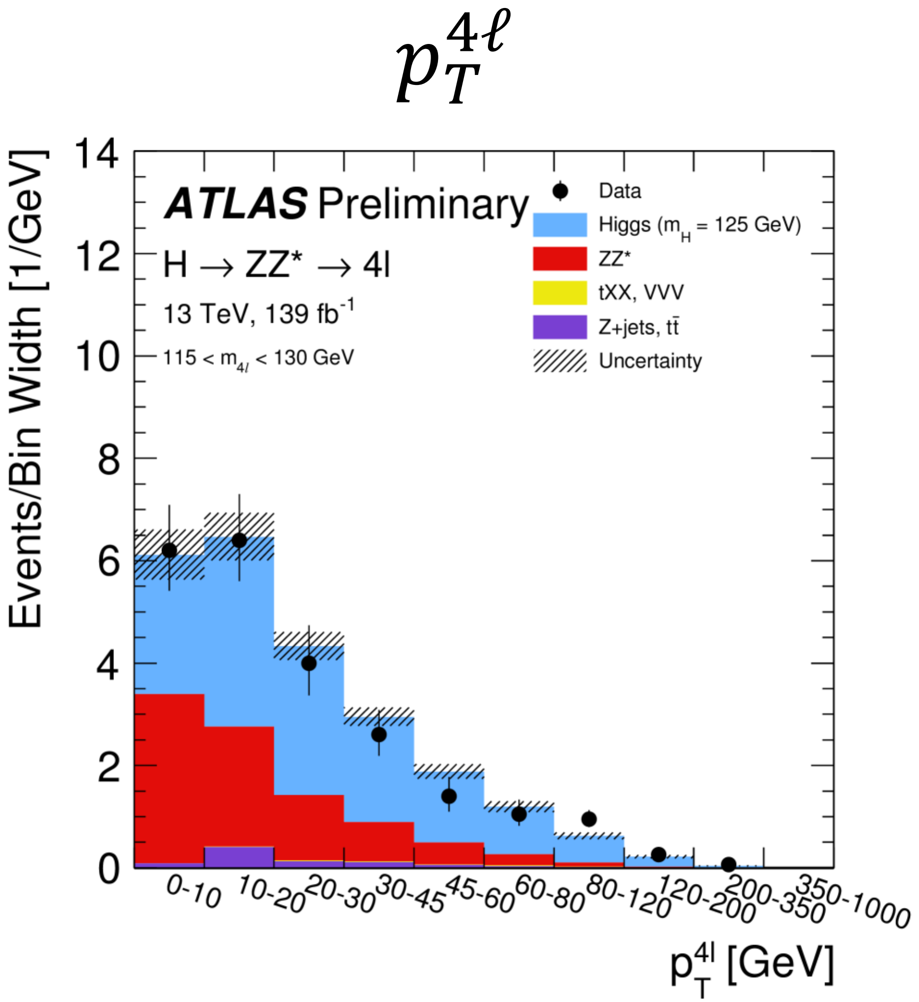

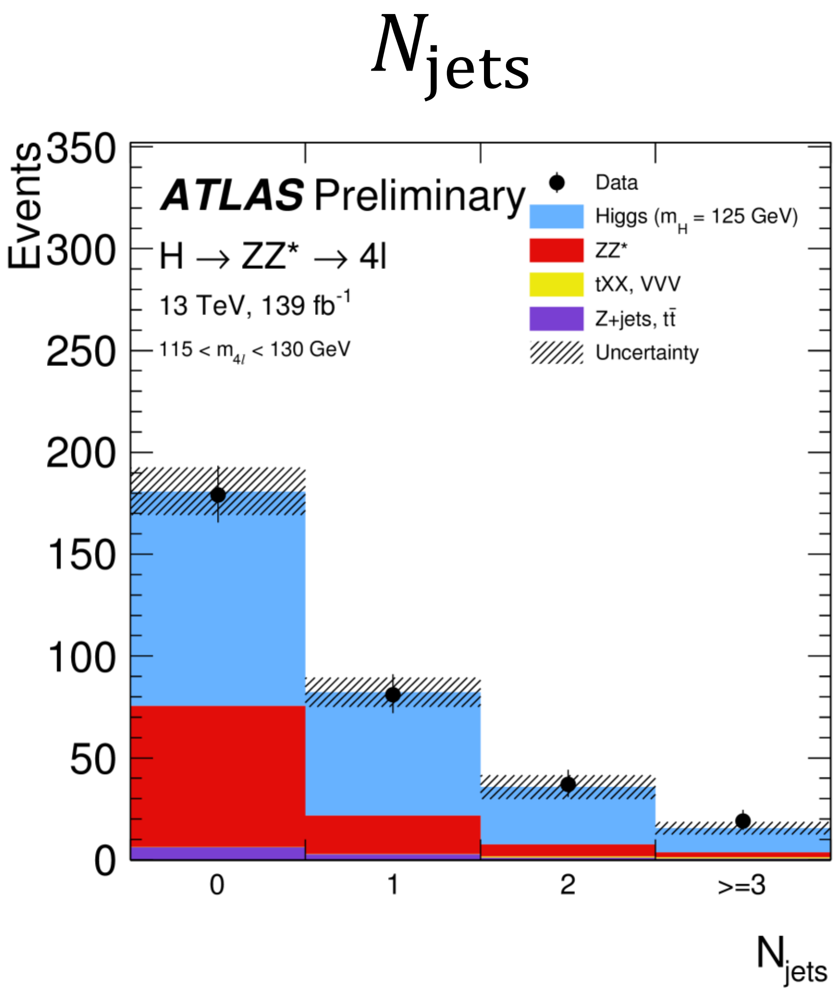

These distributions are pre-fit.

Neural network output distributions (1)

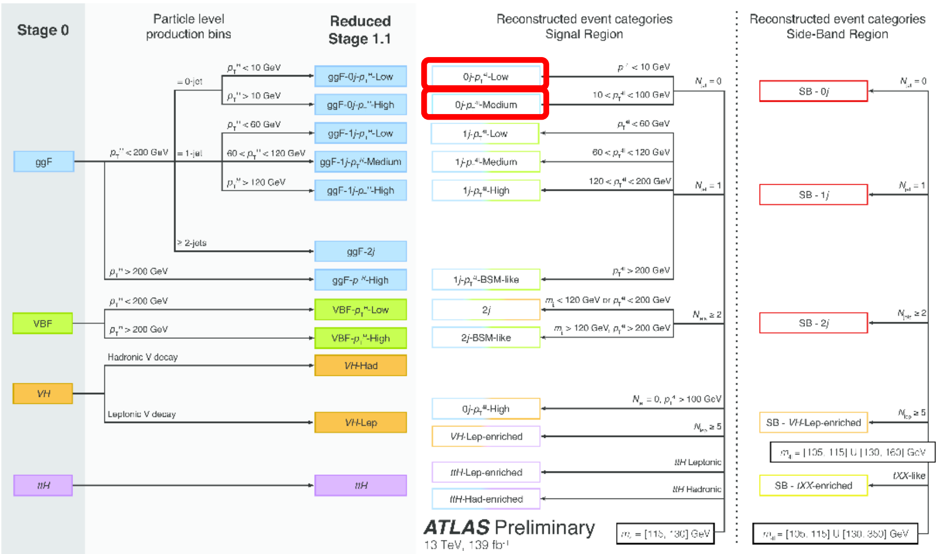

- The expected and observed (pre-fit) distributions of the NN discriminants are shown.
- To separate ggF and ZZ*
- The expected event yields are in reasonable agreement with the observed ones.

$0j$ - $p_T^{4\ell}$ - Low

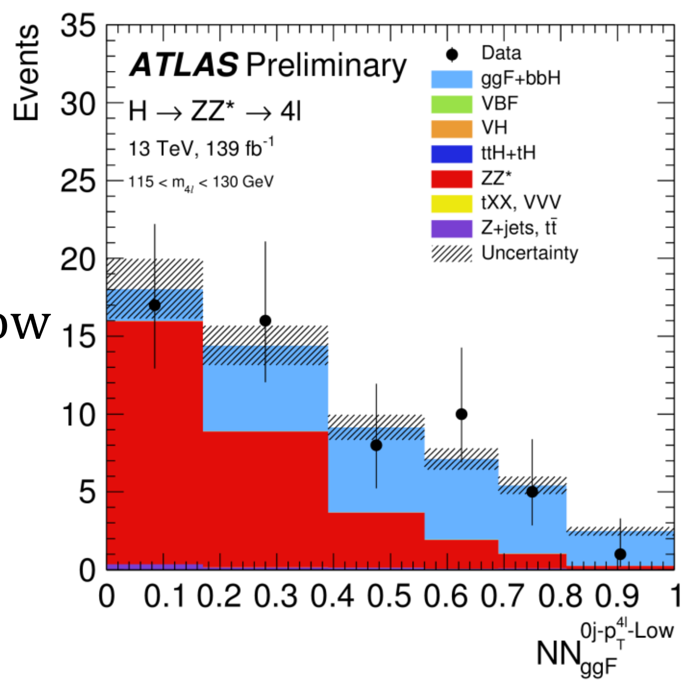

$0j$ - $p_T^{4\ell}$ - Med

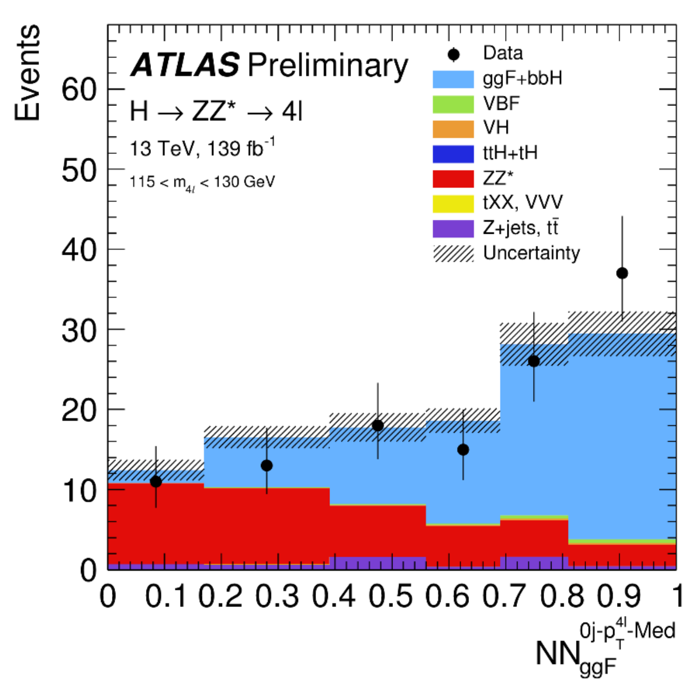

Neural network output distributions (2)

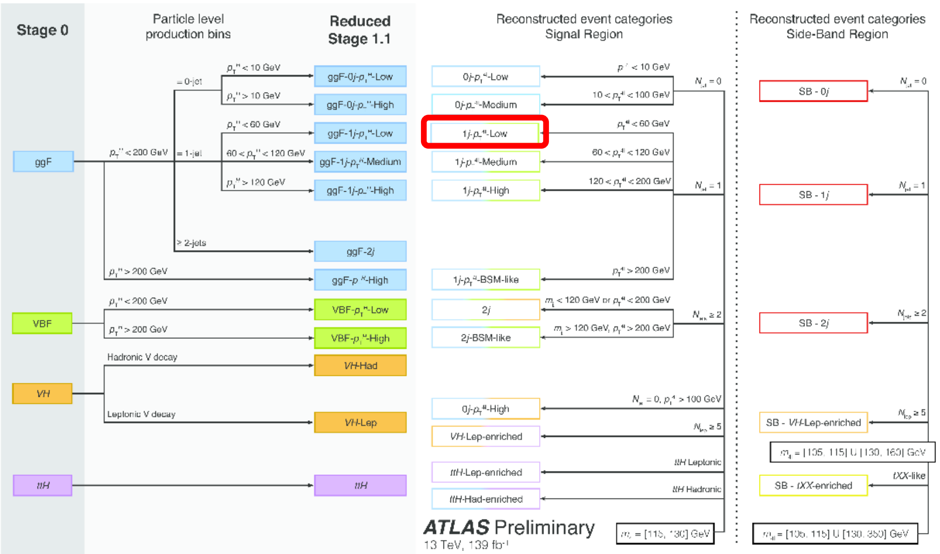

- $1j\text{-}p_T^{4\ell}$-Low category
- Discriminants to separate
  - ggF, VBF, ZZ*

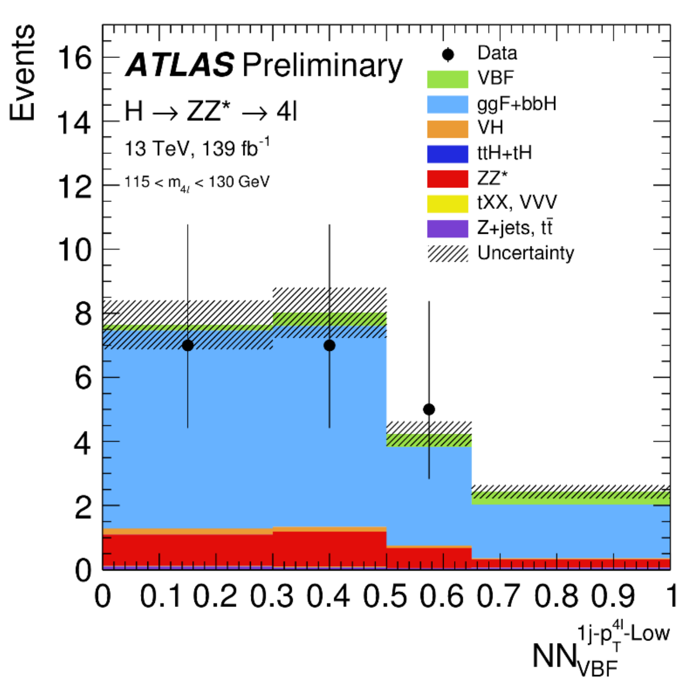

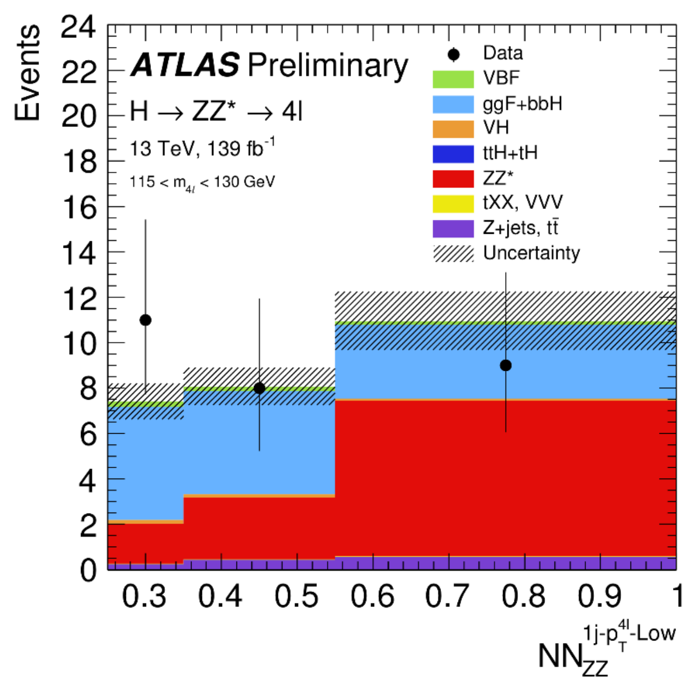

Neural network output distributions (3)

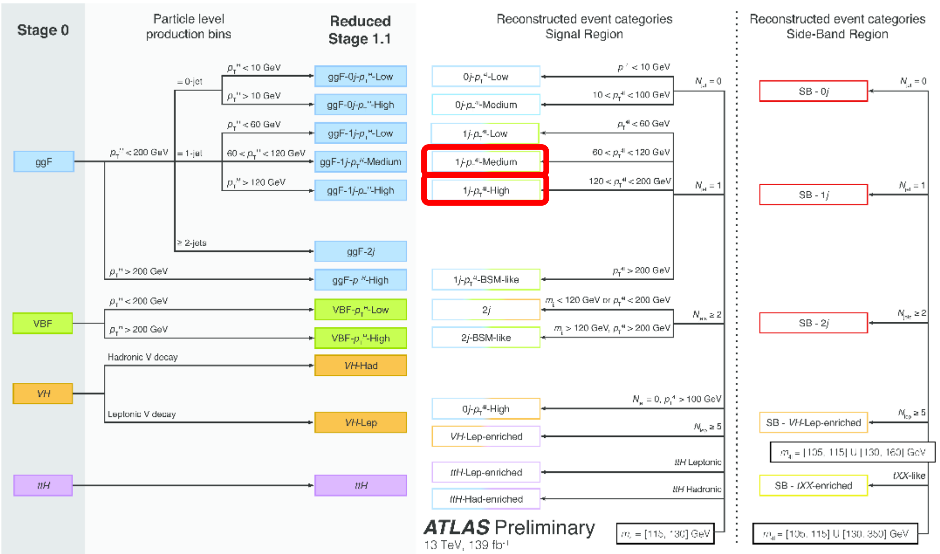

- $1\text{j-}p_{\mathrm{T}}^{4\ell}$-Med category
  - ggF, VBF, ZZ*
- $1\text{j-}p_{\mathrm{T}}^{4\ell}$-High category
  - ggF, VBF

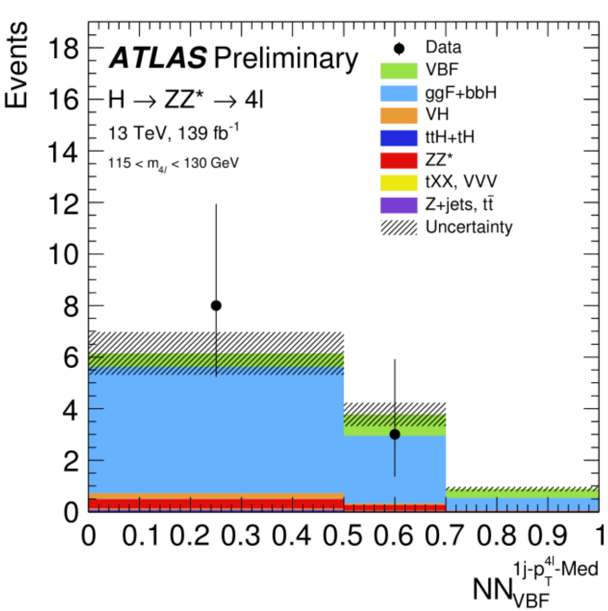

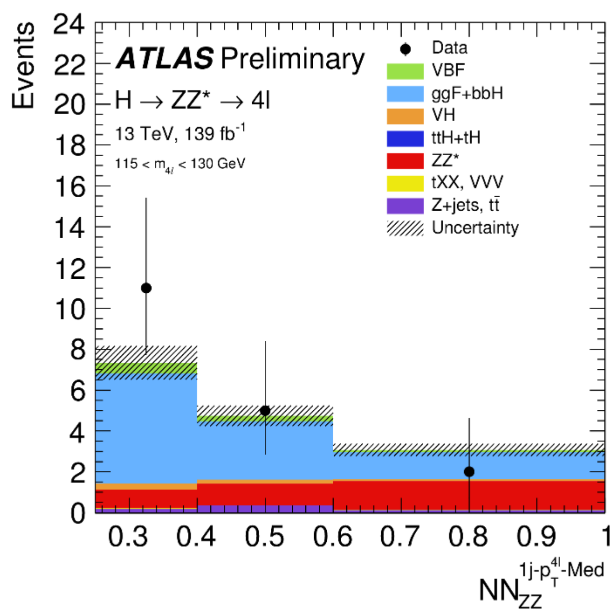

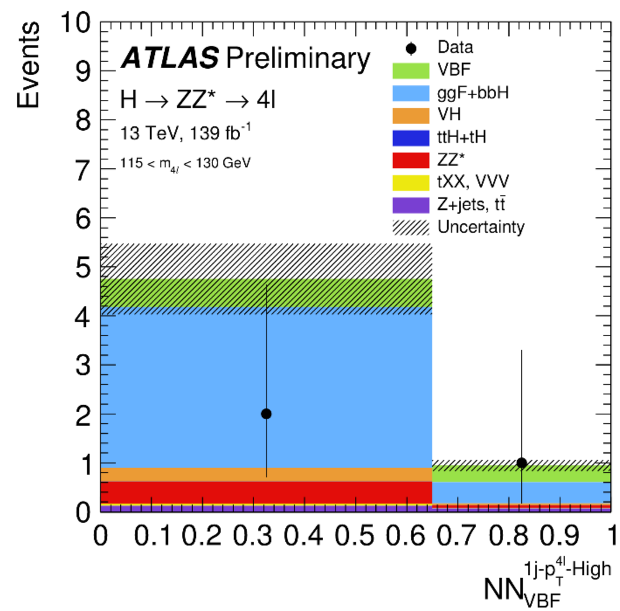

Neural network output distributions (4)

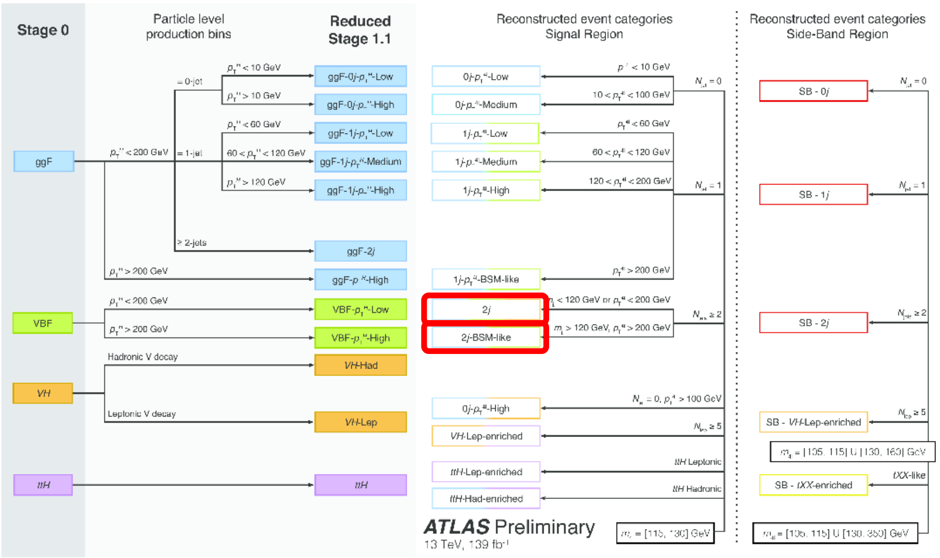

- 2j category
  - ggF, VBF, VH
- 2j-BSM-like category
  - ggF, VBF

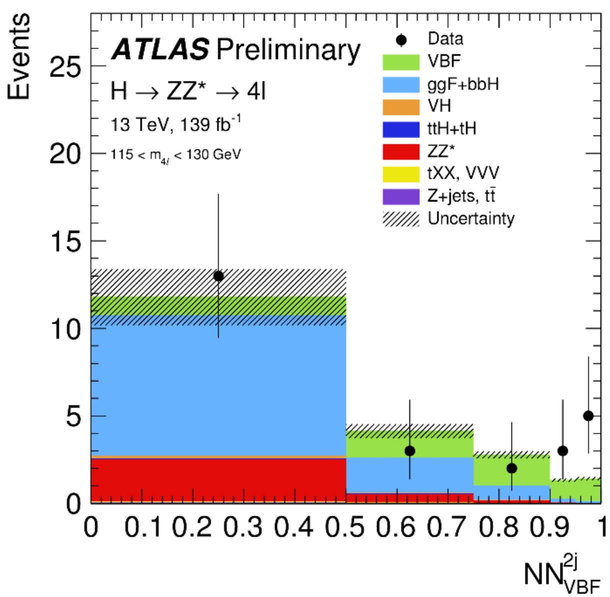

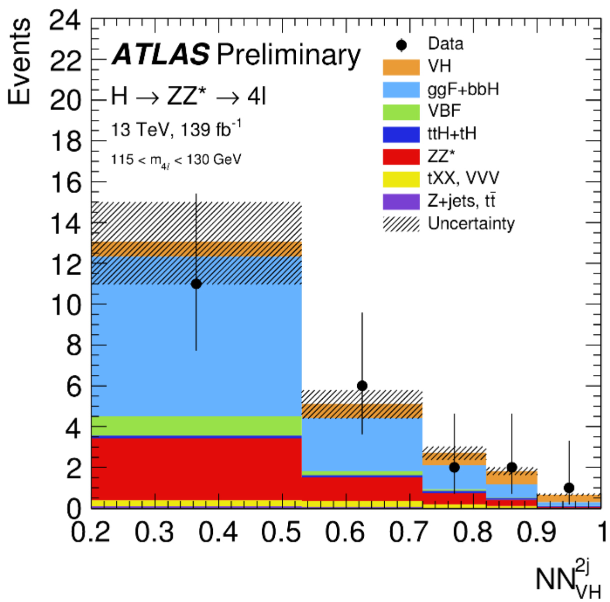

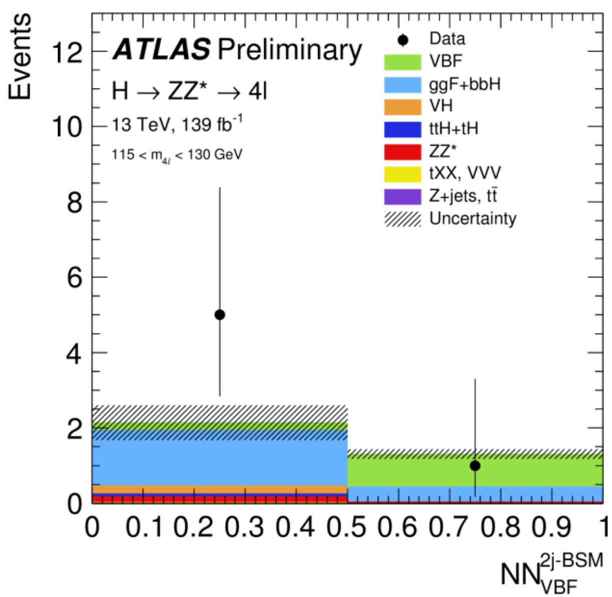

Neural network output distributions (5)

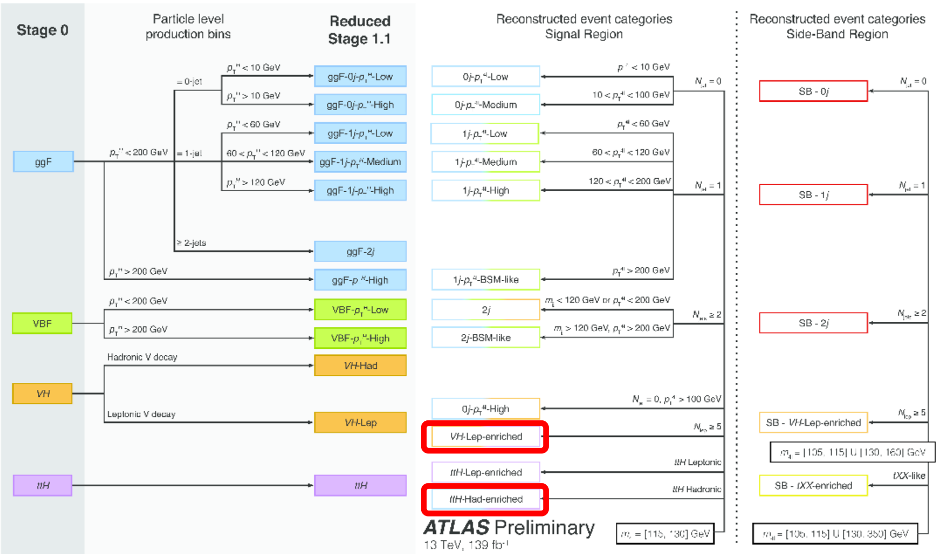

- *ttH*-Had-enriched category
  - ggF, ttH, tXX
- *VH*-Lep-enriched category
  - ttH, VH

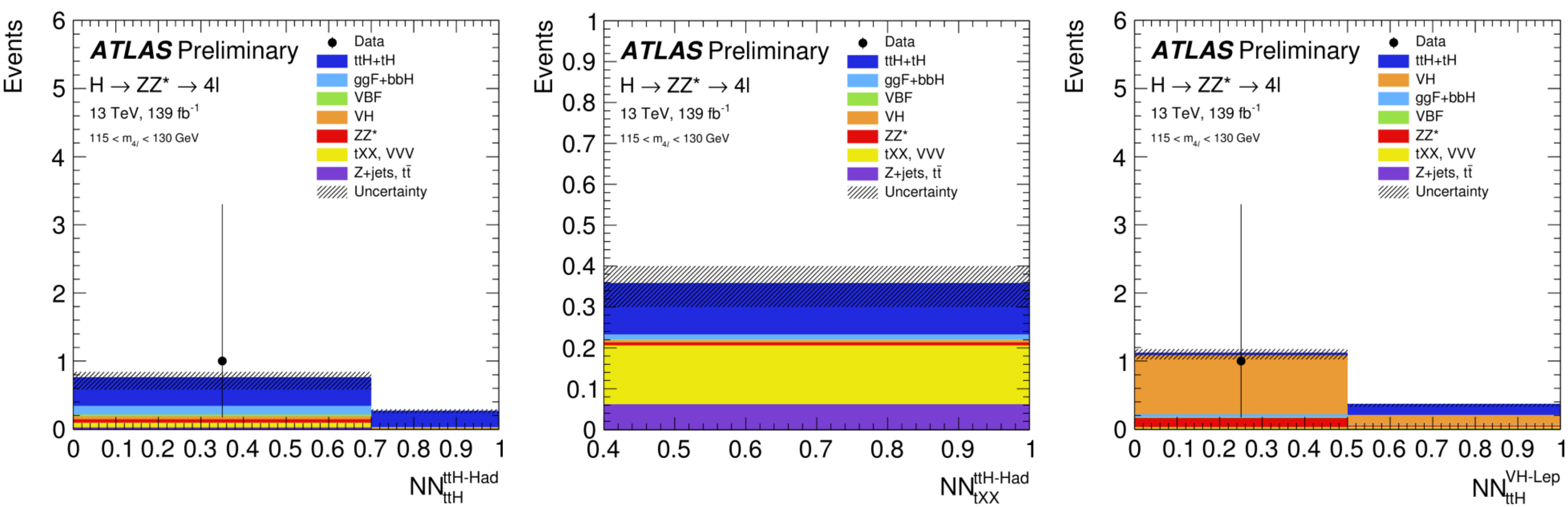

Categories without NN discriminant

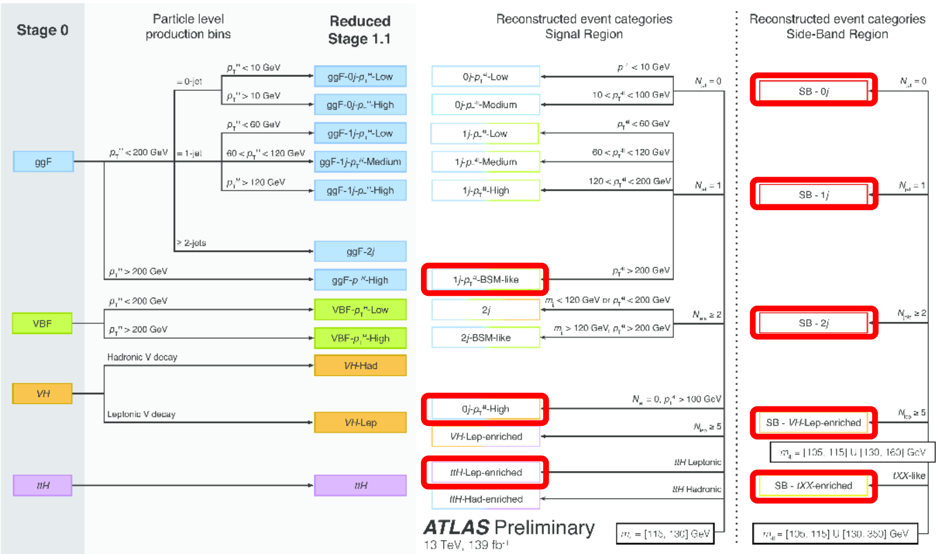

- 0j-$p_{\mathrm{T}}^{4\ell}$-High
- 1j-$p_{\mathrm{T}}^{4\ell}$-BSM-like
- ttH-Lep-enriched
- Sideband
  - 0j, 1j, 2j, tXX, VH-Lep

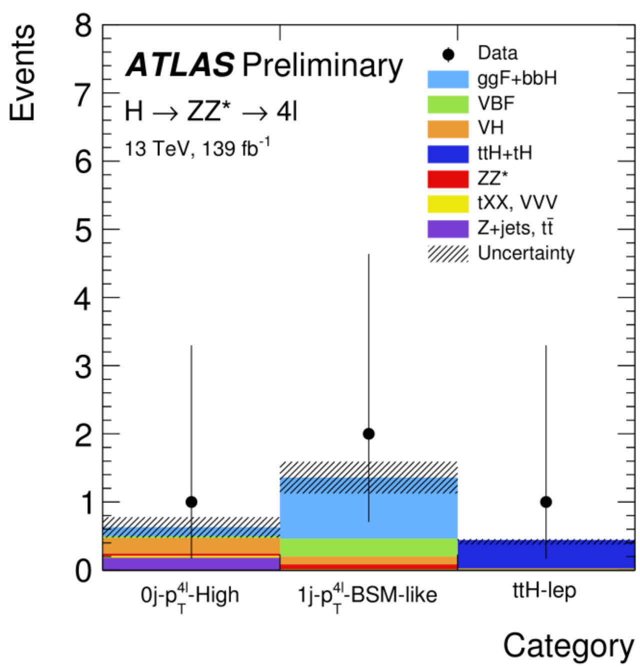

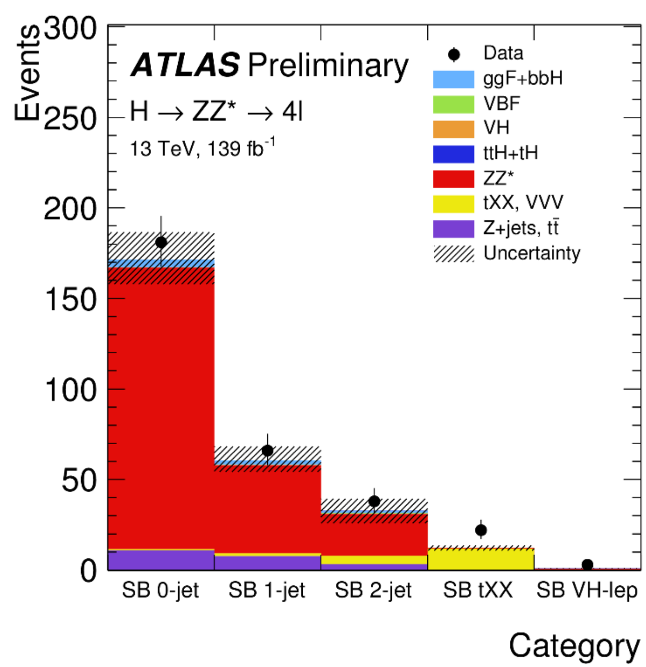

$Z(\rightarrow 2\mu)H(\rightarrow 2e2\mu)$ candidate

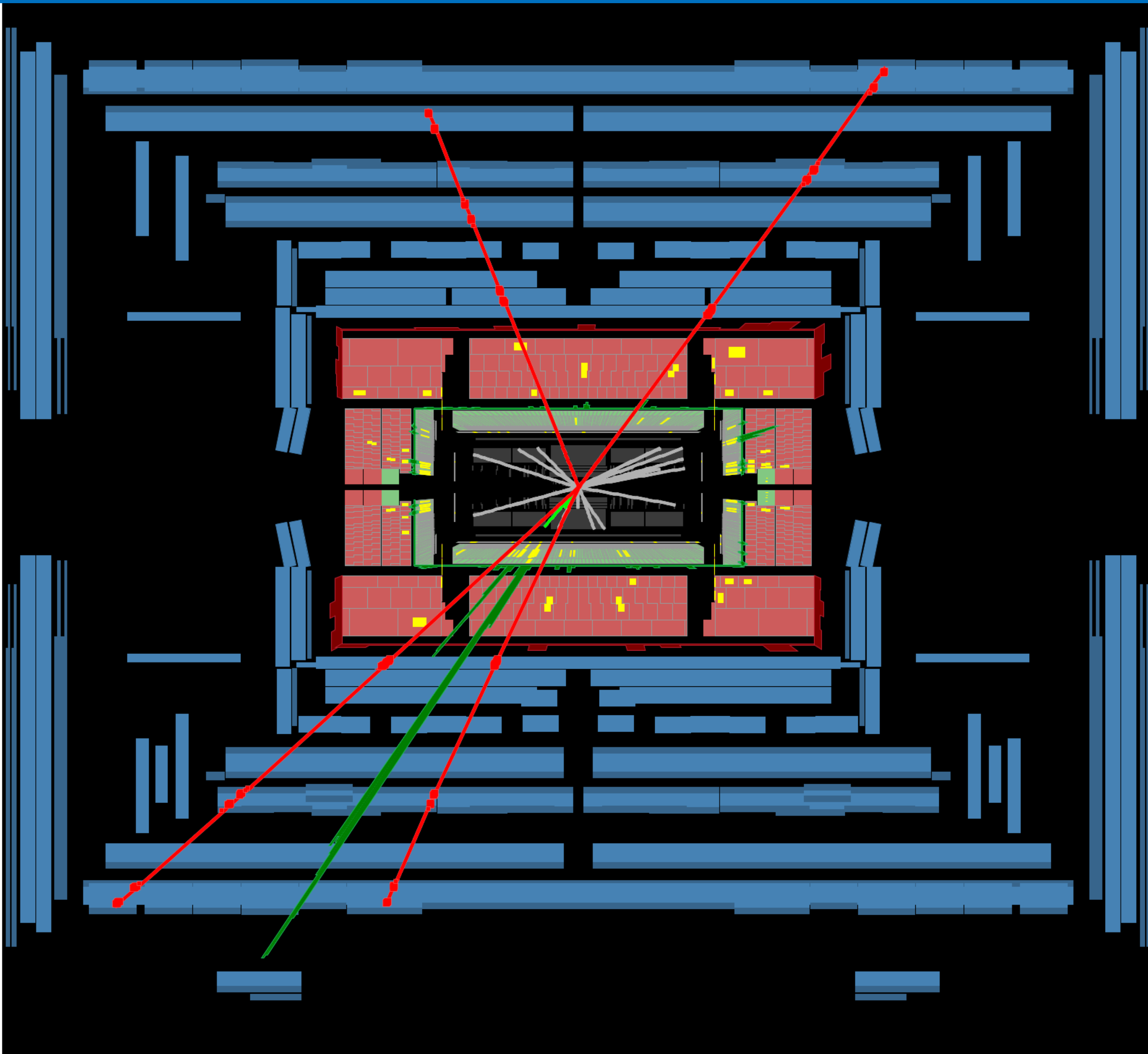

ATLAS EXPERIMENT

Run Number: 359058, Event Number: 2965933740

Date: 2018-08-25 02:51:44 CEST

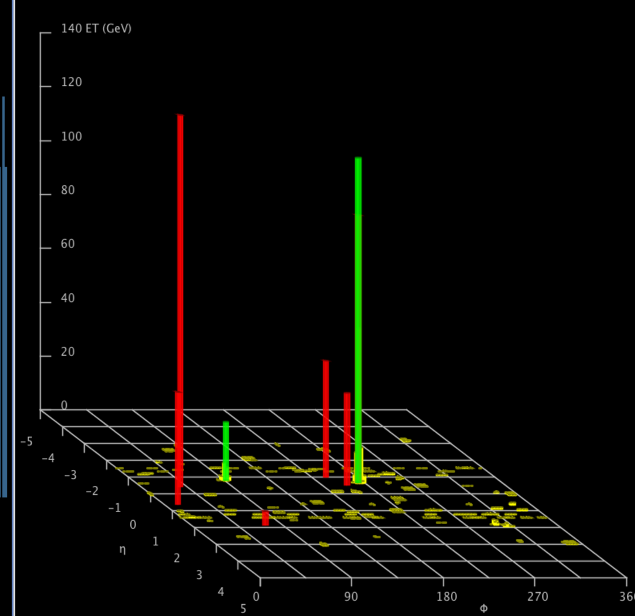

Invariant mass of the extra di-muon in the upper hemisphere is 91.5 GeV.

$Z(\to 2\nu)$ or $W(\to \ell\nu)H(\to 2\mu 2e)$ candidate

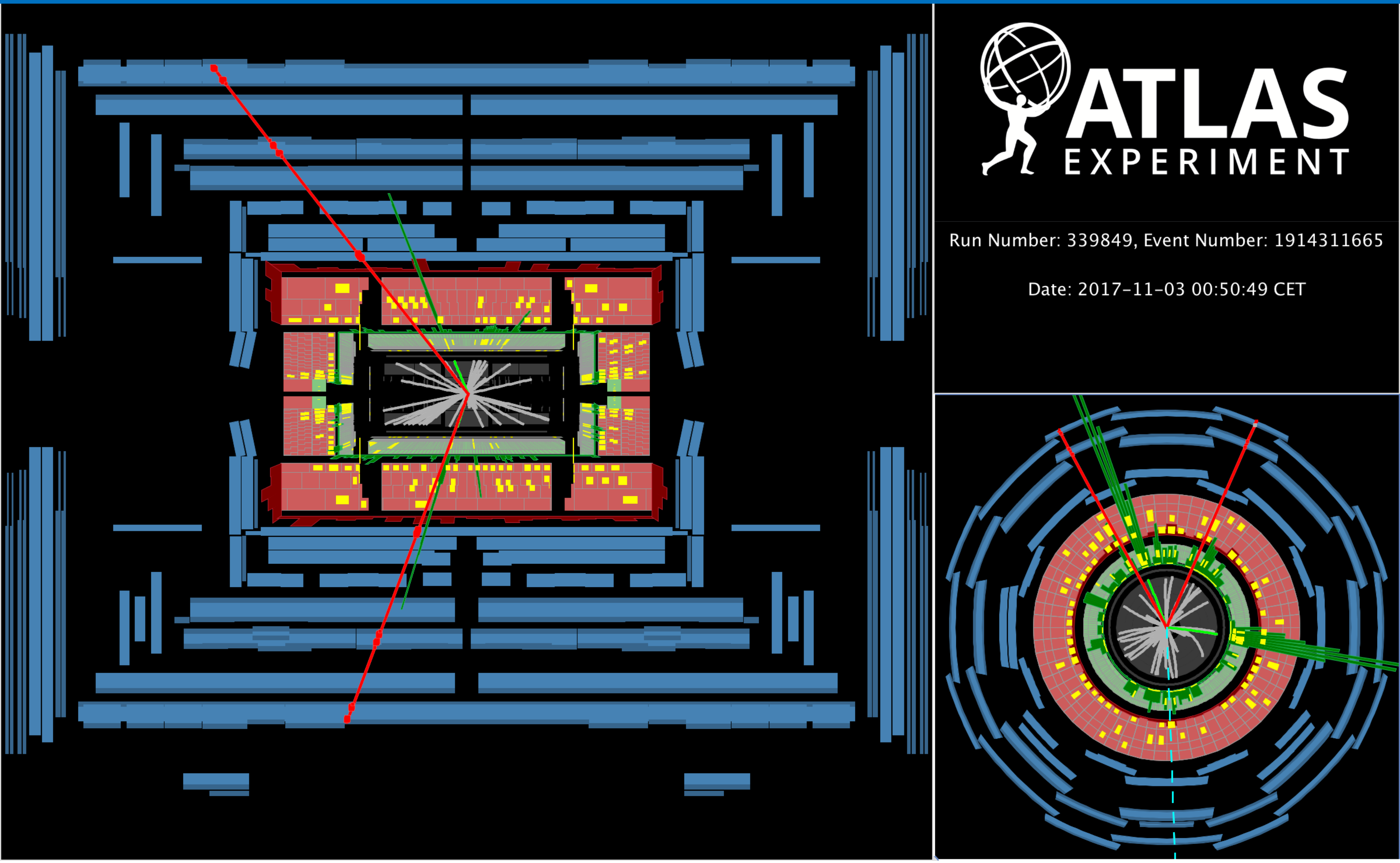

MET is 240.3 GeV. $p_T^{4\ell}$ is 181.1 GeV. They are back-to-back ($\Delta\phi$=3.10).

Fiducial and total cross sections

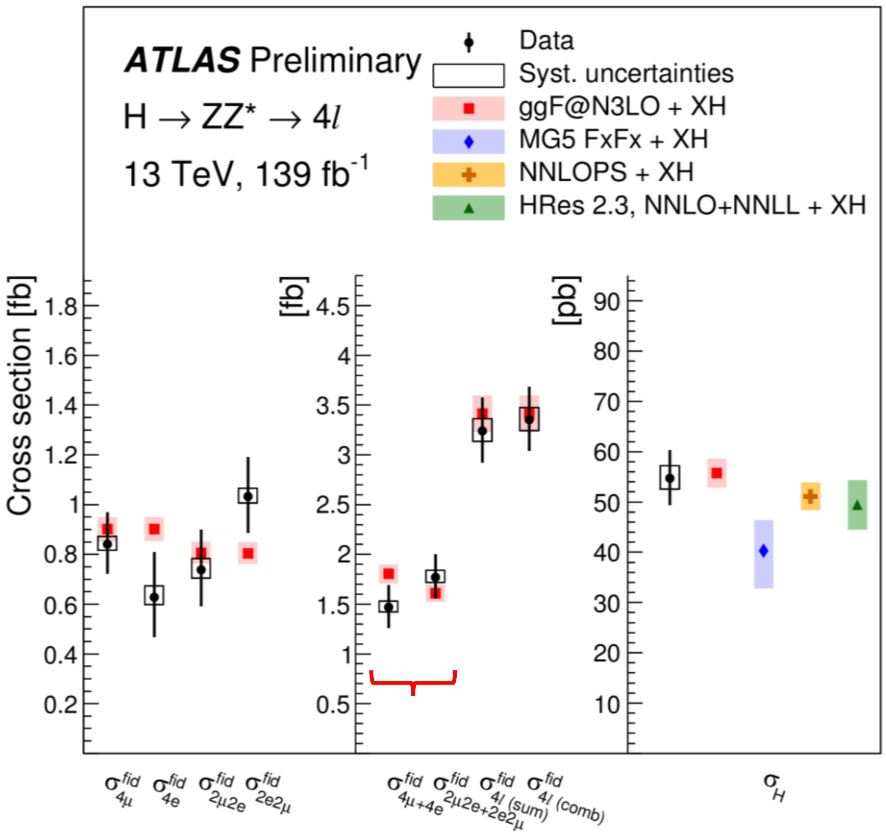

Cross section [fb]	Data	± (stat.)	± (syst.)	Standard Model prediction	p-value [%]
$\sigma_{4\mu}$	0.84	±0.12	±0.03	0.901(48)	63
σ_{4e}	0.63	±0.17	±0.04	0.901(48)	14
$\sigma_{2\mu 2e}$	0.74	±0.15	±0.04	0.805(43)	66
$\sigma_{2e2\mu}$	1.03	±0.15	±0.03	0.805(43)	11
$\sigma_{4\mu+4e}$	1.47	±0.21	±0.06	1.80(10)	14
$\sigma_{2\mu 2e+2e2\mu}$	1.77	±0.21	±0.06	1.61(9)	46
σ_{sum}	3.24	±0.31	±0.11	3.41(18)	60
σ_{comb}	3.35	±0.30	±0.12	3.41(18)	85
σ_{tot} [pb]	54.7	±4.9	±2.3	55.7(28)	85

- Same-flavor cross sections should be about 10% higher than mixed-flavor cross section due to EW corrections.
- We are not quite sensitive to this yet.
  - About 14% uncertainty

- The fiducial cross section is extrapolated to the total phase space.
- The total cross section is compared to the cross sections predicted by N^3LO, MadGraph5_aMC@NLO-FxFx (MG5-FxFx), NNLOPS and Hres 2.3 for ggF.

Differential cross sections

$p_T^{4\ell}$

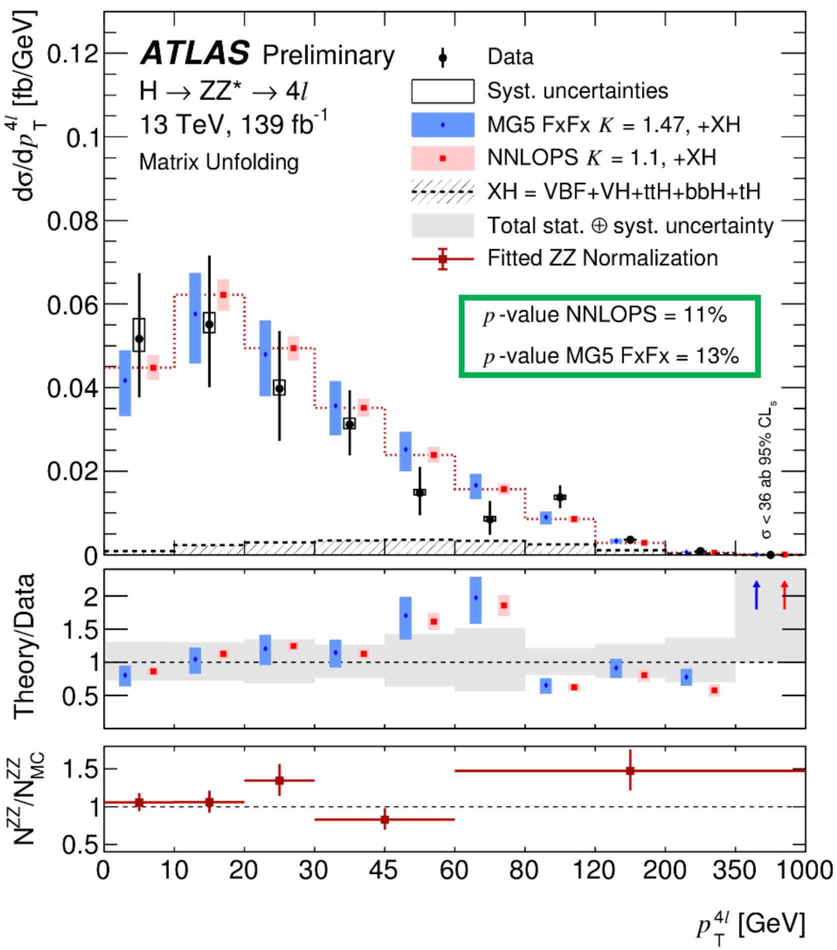

N_{jets}

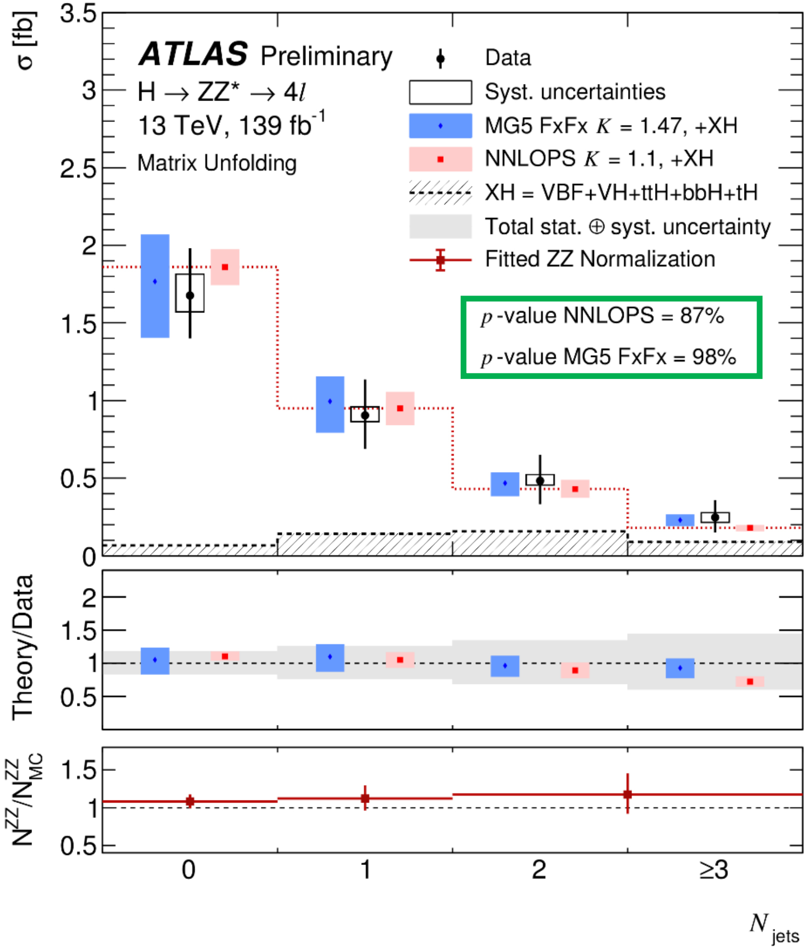

- All samples are normalized to the most accurate SM predictions.
- Fitted values of ZZ^* background normalization factors are also shown.
- Good agreement is found between the data and the predictions of the SM.

Cross section ratio and signal strength

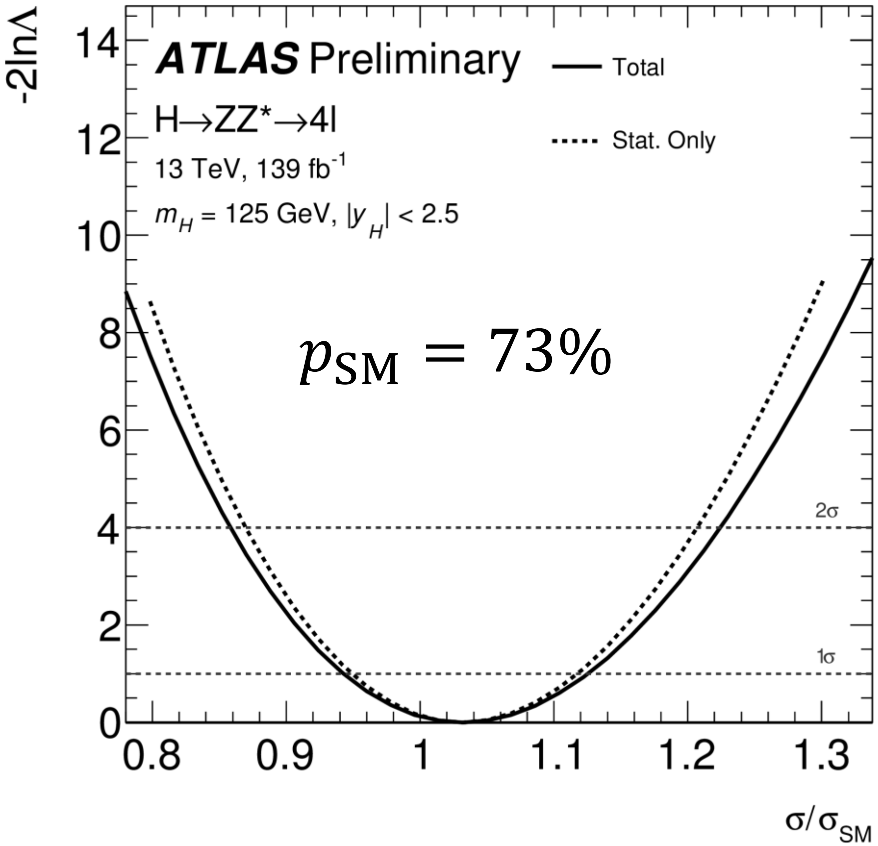

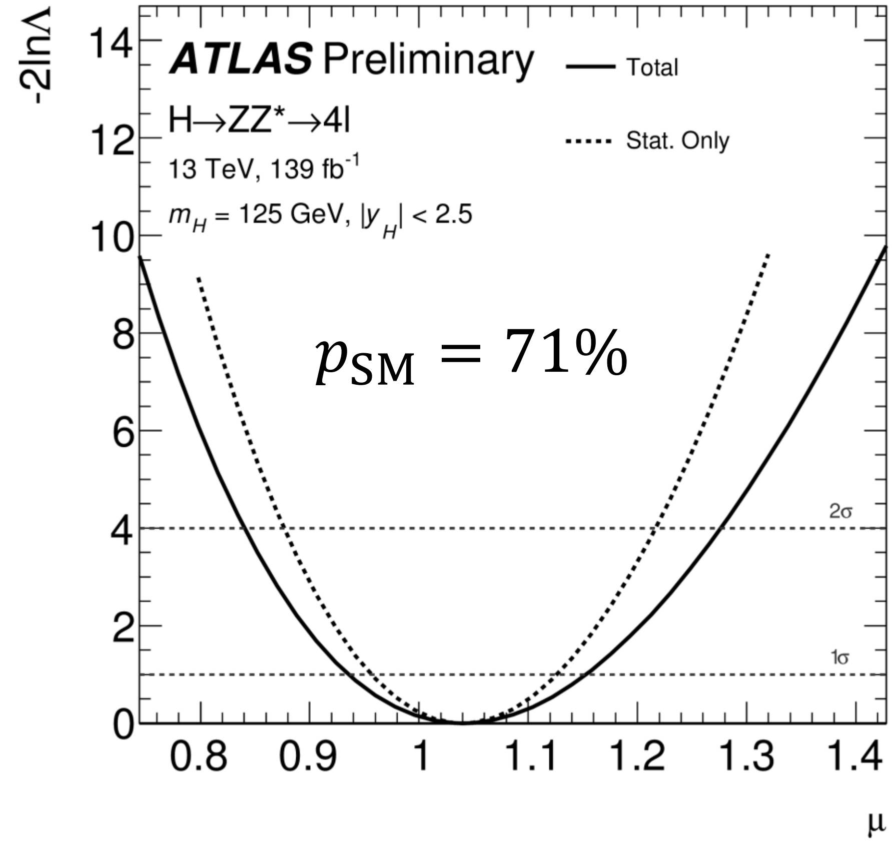

$$\sigma \cdot \mathcal{B} \equiv \sigma \cdot \mathcal{B}(H \to ZZ^*) = 1.38 \pm 0.11(\text{stat.})^{+0.05}_{-0.03}(\text{exp.}) \pm 0.03(\text{th.})\ \text{pb} = 1.38 \pm 0.12\ \text{pb}.$$

$$(\sigma \cdot \mathcal{B})_{\text{SM}} \equiv (\sigma \cdot \mathcal{B}(H \to ZZ^*))_{\text{SM}} = 1.33 \pm 0.09\ \text{pb}.$$

$$\mu = 1.04^{+0.09}_{-0.08}(\text{stat.})^{+0.04}_{-0.03}(\text{exp.})^{+0.06}_{-0.05}(\text{th.}) = 1.04^{+0.12}_{-0.10}.$$

$\sigma \cdot \mathcal{B}(H \to ZZ^*)/[\sigma \cdot \mathcal{B}\,(H \to ZZ^*)]_{SM}$

Stage 0

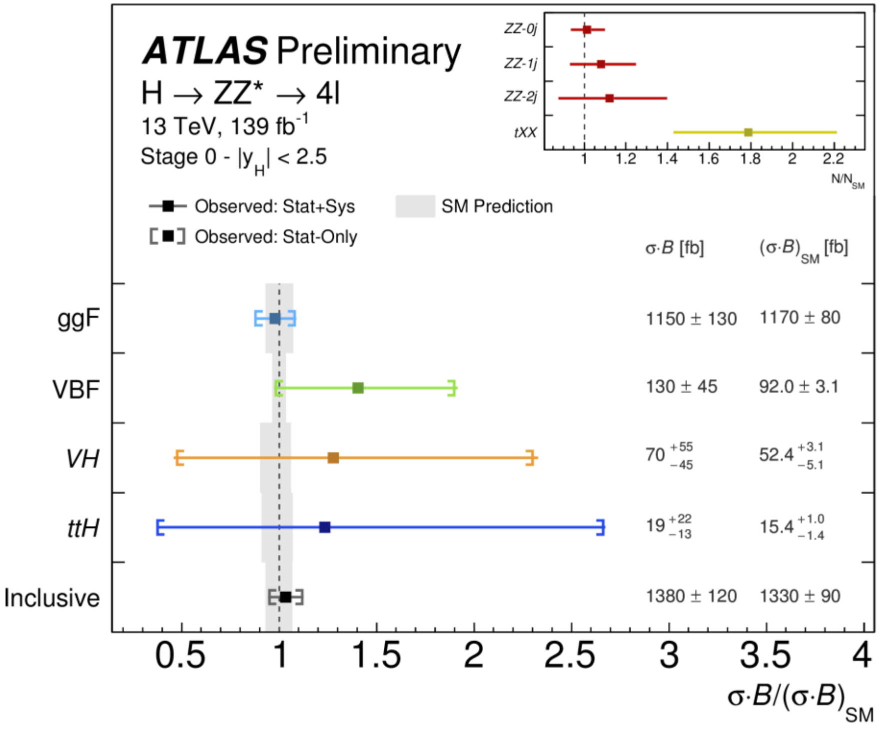

Reduced Stage 1.1

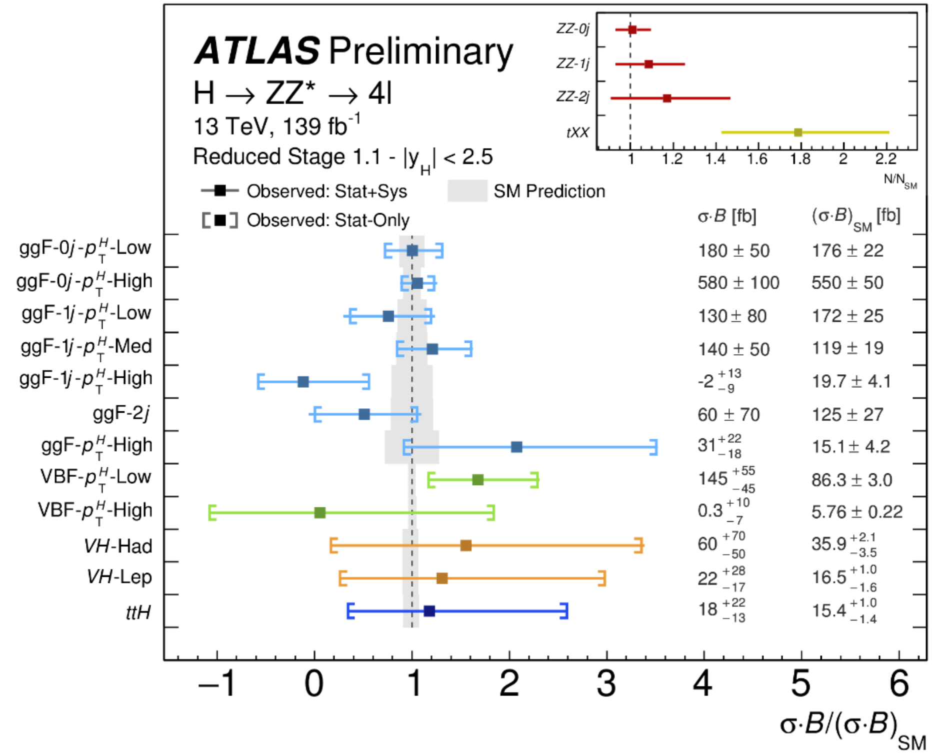

All Stage 0 and reduced Stage 1.1 ggF measurements agree with the predictions for the SM Higgs boson within 1.5 standard deviation.

Summary

- Inclusive fiducial, differential and production mode cross section measurements of Higgs boson in the $H \rightarrow ZZ^* \rightarrow 4\ell$ decay channel are presented.
- They are based on 139 fb^{-1} of $\sqrt{s}$=13 TeV proton-proton collisions recorded by the ATLAS detector at the LHC in 2015—2018.
- Inclusive fiducial cross section
  - $\sigma_{\text{fid}} = 3.35 \pm 0.30\ (\text{stat.}) \pm 0.12\ (\text{syst.})\ \text{fb}$
  - $\sigma_{\text{fid,SM}} = 3.41 \pm 0.18\ \text{fb}$
- Differential cross sections as a function of $p_T^{4\ell}$ and N_{jets}
  - Good agreement is found between the data and the predictions of the SM.
- ggF production cross section times branching ratio
  - $\sigma_{\text{ggF}} \cdot \mathcal{B}(H \rightarrow ZZ^*) = 1.15 \pm 0.12\ (\text{stat.}) \pm 0.04\ (\text{exp.}) \pm 0.03\ (\text{th.})\ \text{pb}$
  - $\left[\sigma_{\text{ggF}} \cdot \mathcal{B}\ (H \rightarrow ZZ^*)\right]_{\text{SM}} = 1.17 \pm 0.08\ \text{pb}$

Backup slides

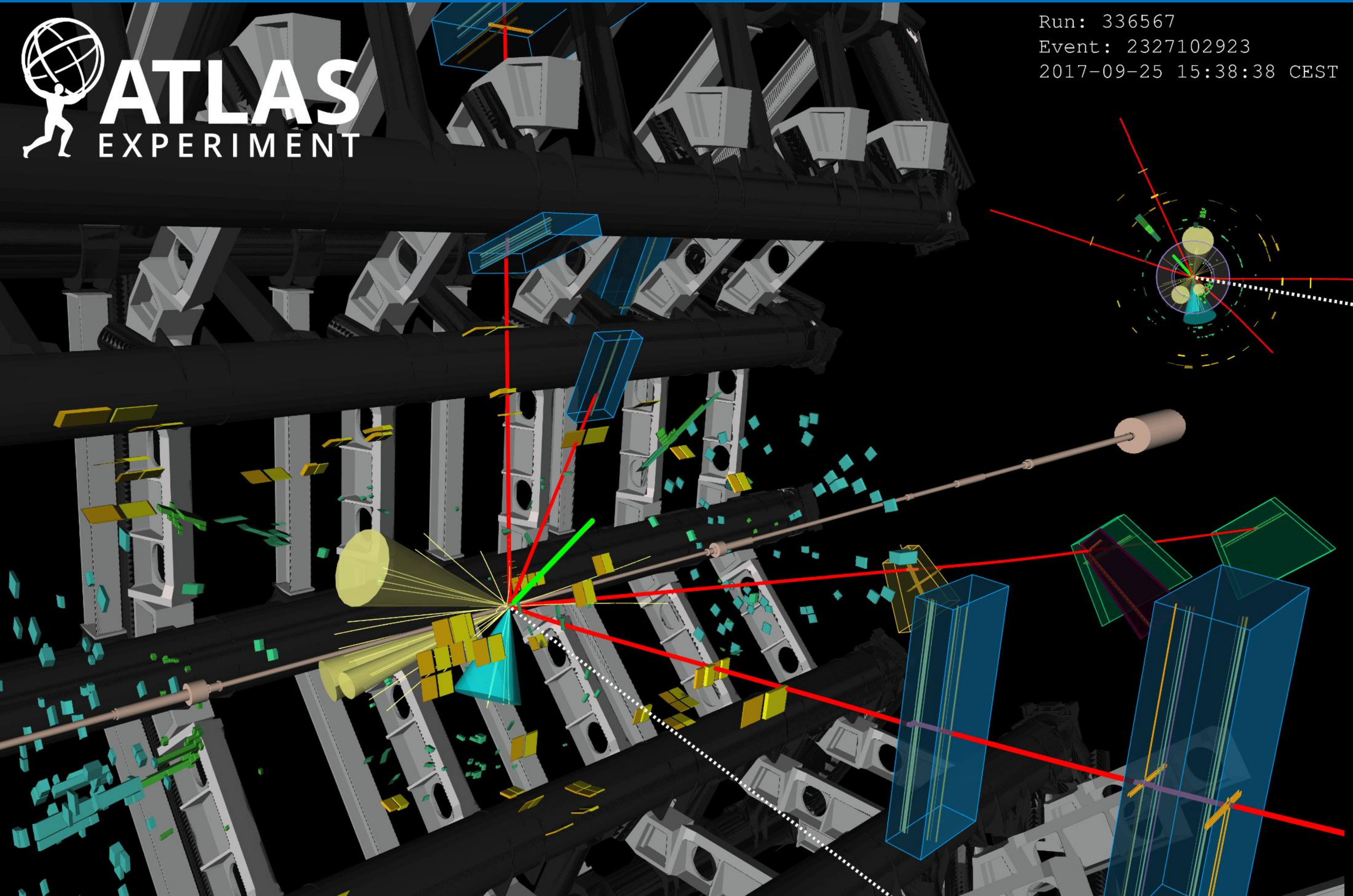

12+3 minute talk

- Title: Measurement of cross sections in Higgs boson decays to four leptons with the ATLAS detector

- Abstract: Higgs boson decays to four leptons can be selected with a very high purity and are very well suited for measurements of Higgs boson properties, despite the small $H\rightarrow ZZ\rightarrow 4l$ branching ratio. This talk will present measurements of differential cross sections, as well as cross section measurements for the different Higgs boson production processes in the simplified template cross section framework using pp collision data collected at 13 TeV.

Fiducial and differential XS strategy

- **Goal: model independent measurements of Higgs differential fiducial and inclusive cross sections (XS)**
  - Fiducial selection follows closely reconstruction-level selection
  - Unfold to correct for detector resolution and efficiency effects
- Template fit of $m_{4\ell}$ distribution to extract the number of signal events
- Use likelihood fit including detector response matrix for unfolding as the baseline method.
  - Bin-by-bin correction factor unfolding is alternative.
- $N_i(m_{4\ell}) = \sum_j r_{ij} \cdot \left(1 + f_i^{\text{nonfid}}\right) \cdot \sigma_j^{\text{fid}} \cdot P(m_{4\ell}) \cdot \mathcal{L} + N_i^{\text{bkg}}(m_{4\ell})$
- $\sigma_j^{\text{fid}} = \sigma_j \cdot A_j \cdot \mathcal{B}(H \to ZZ^* \to 4\ell)$
  - N_i : number of expected events in observable bin i
  - P : shape of signal contribution (from MC)
  - $\mathcal{L}$: integrated luminosity
  - A_i : acceptance in fiducial phase space
  - σ_i : total cross section
  - N_i^{bkg} : background contribution
  - r_{ij} : detector response matrix, generated in bin j and reconstructed in bin i
  - f_i^{nonfid}: correction for reconstructed but not in fiducial phase space

Expected number of SM Higgs events (Stage 0)

For $m_H = 125$ GeV at an integrated luminosity 139 fb^{-1} and $\sqrt{s} = 13$ TeV

Reconstructed event category	SM Higgs boson production mode ggF	VBF	WH	ZH	ttH + tH	bbH
Signal			$115 < m_{4\ell} < 130$ GeV			
$0j$-$p_{\mathrm{T}}^{4\ell}$-Low	24.6 ± 3.1	0.077 ± 0.010	0.0194 ± 0.0035	0.0131 ± 0.0024	–	0.18 ± 0.09
$0j$-$p_{\mathrm{T}}^{4\ell}$-Med	76 ± 8	1.18 ± 0.14	0.39 ± 0.05	0.36 ± 0.04	–	0.8 ± 0.4
$0j$-$p_{\mathrm{T}}^{4\ell}$-High	0.132 ± 0.032	0.0302 ± 0.0033	0.064 ± 0.006	0.161 ± 0.015	0.00065 ± 0.00025	–
$1j$-$p_{\mathrm{T}}^{4\ell}$-Low	30 ± 4	2.03 ± 0.11	0.52 ± 0.05	0.306 ± 0.031	0.0074 ± 0.0016	0.40 ± 0.20
$1j$-$p_{\mathrm{T}}^{4\ell}$-Med	17.5 ± 2.8	2.65 ± 0.16	0.52 ± 0.05	0.354 ± 0.035	0.0087 ± 0.0020	0.09 ± 0.05
$1j$-$p_{\mathrm{T}}^{4\ell}$-High	3.7 ± 0.8	0.93 ± 0.07	0.167 ± 0.014	0.154 ± 0.013	0.0047 ± 0.0011	0.012 ± 0.006
$1j$-$p_{\mathrm{T}}^{4\ell}$-BSM-Like	0.90 ± 0.23	0.268 ± 0.019	0.065 ± 0.010	0.052 ± 0.008	0.0017 ± 0.0006	0.0008 ± 0.0004
$2j$	23 ± 5	8.0 ± 0.5	1.86 ± 0.14	1.44 ± 0.11	0.47 ± 0.05	0.28 ± 0.14
$2j$-BSM-like	1.9 ± 0.6	1.05 ± 0.05	0.119 ± 0.013	0.110 ± 0.012	0.078 ± 0.007	0.0027 ± 0.0014
VH-Lep-enriched	0.046 ± 0.017	0.0191 ± 0.0031	0.80 ± 0.06	0.211 ± 0.017	0.172 ± 0.015	0.0026 ± 0.0013
ttH-Had-enriched	0.13 ± 0.13	0.0162 ± 0.0033	0.0142 ± 0.0024	0.044 ± 0.007	0.73 ± 0.08	0.017 ± 0.009
ttH-Lep-enriched	0.0008 ± 0.0012	0.00019 ± 0.00014	0.0039 ± 0.0024	0.0023 ± 0.0014	0.40 ± 0.04	–
Sideband			$105 < m_{4\ell} < 115$ GeV or $130 < m_{4\ell} < 160$ GeV			
SB-$0j$	4.4 ± 0.5	0.058 ± 0.009	0.103 ± 0.012	0.040 ± 0.005	–	0.046 ± 0.024
SB-$1j$	2.30 ± 0.29	0.256 ± 0.023	0.100 ± 0.011	0.060 ± 0.006	0.0056 ± 0.0012	0.021 ± 0.011
SB-$2j$	1.17 ± 0.25	0.40 ± 0.05	0.116 ± 0.014	0.089 ± 0.010	0.109 ± 0.010	0.016 ± 0.008
SB-VH-Lep-enriched	0.019 ± 0.008	0.0029 ± 0.0010	0.086 ± 0.008	0.090 ± 0.008	0.066 ± 0.007	0.0013 ± 0.0007
			$105 < m_{4\ell} < 115$ GeV or $130 < m_{4\ell} < 350$ GeV			
SB-tXX-enriched	0.0009 ± 0.0015	0.00015 ± 0.00015	0.00042 ± 0.00016	0.00041 ± 0.00016	0.064 ± 0.008	0.00008 ± 0.00008
Total	186 ± 14	17.0 ± 0.8	5.0 ± 0.4	3.48 ± 0.25	2.12 ± 0.18	1.9 ± 1.0

Expected and observed numbers of events

Reconstructed event category	Signal	ZZ^* background	tXX background	Other backgrounds	Total expected	Observed
Signal			$115 < m_{4\ell} < 130$ GeV			
$0j$-$p_{\mathrm{T}}^{4\ell}$-Low	24.9 ± 3.1	31 ± 4	–	0.78 ± 0.11	57 ± 5	57
$0j$-$p_{\mathrm{T}}^{4\ell}$-Med	79 ± 8	38 ± 5	0.047 ± 0.009	5.2 ± 0.5	123 ± 10	120
$0j$-$p_{\mathrm{T}}^{4\ell}$-High	0.39 ± 0.04	0.033 ± 0.015	0.011 ± 0.004	0.182 ± 0.031	0.63 ± 0.05	1
$1j$-$p_{\mathrm{T}}^{4\ell}$-Low	33 ± 4	14.3 ± 2.6	0.088 ± 0.007	1.52 ± 0.22	49 ± 5	47
$1j$-$p_{\mathrm{T}}^{4\ell}$-Med	21.2 ± 2.8	4.0 ± 0.6	0.114 ± 0.010	0.77 ± 0.14	26.0 ± 2.8	29
$1j$-$p_{\mathrm{T}}^{4\ell}$-High	5.0 ± 0.8	0.50 ± 0.09	0.047 ± 0.007	0.189 ± 0.030	5.7 ± 0.8	3
$1j$-$p_{\mathrm{T}}^{4\ell}$-BSM-Like	1.28 ± 0.23	0.072 ± 0.033	0.006 ± 0.004	0.040 ± 0.008	1.41 ± 0.23	2
$2j$	35 ± 5	8.2 ± 2.4	0.96 ± 0.08	0.23 ± 0.06	45 ± 5	48
$2j$-BSM-like	3.2 ± 0.6	0.18 ± 0.06	0.032 ± 0.005	1.20 ± 0.11	4.6 ± 0.6	6
VH-Lep-enriched	1.25 ± 0.07	0.159 ± 0.020	0.037 ± 0.008	0.0052 ± 0.0031	1.47 ± 0.07	1
ttH-Had-enriched	0.95 ± 0.16	0.063 ± 0.025	0.225 ± 0.031	0.09 ± 0.04	1.32 ± 0.17	1
ttH-Lep-enriched	0.41 ± 0.04	–	0.0130 ± 0.0013	–	0.42 ± 0.04	1
Sideband			$105 < m_{4\ell} < 115$ GeV or $130 < m_{4\ell} < 160$ GeV			
SB-$0j$	4.6 ± 0.5	155 ± 14	0.22 ± 0.05	12.6 ± 1.8	173 ± 14	181
SB-$1j$	2.74 ± 0.29	49 ± 6	1.35 ± 0.18	6.4 ± 0.9	59 ± 6	66
SB-$2j$	1.90 ± 0.26	23 ± 6	4.3 ± 0.5	4.4 ± 0.6	34 ± 6	38
SB-VH-Lep-enriched	0.266 ± 0.015	0.49 ± 0.06	0.132 ± 0.020	0.07 ± 0.13	1.06 ± 0.14	3
			$105 < m_{4\ell} < 115$ GeV or $130 < m_{4\ell} < 350$ GeV			
SB-tXX-enriched	0.066 ± 0.008	0.31 ± 0.11	11.6 ± 1.3	0.46 ± 0.13	12.5 ± 1.3	22

The expected numbers are pre-fit.

Expected and observed cross sections

Production bin	Cross section $(\sigma \cdot \mathcal{B})$ [pb]		$(\sigma \cdot \mathcal{B})/(\sigma \cdot \mathcal{B})_{SM}$
	SM expected	Observed	Observed
Inclusive production, $\lvert y_H \rvert < 2.5$			
	1.33 ± 0.09	$1.38 \pm 0.11 \pm 0.04 \pm 0.03$	$1.033 \pm 0.08 \pm 0.03 \pm 0.02$
Stage-0 production bins, $\lvert y_H \rvert < 2.5$			
ggF	1.17 ± 0.08	$1.15 \pm 0.12 \pm 0.04 \pm 0.03$	$0.98 \pm 0.10 \pm 0.03 \pm 0.03$
VBF	0.0920 ± 0.0031	$0.13 \pm 0.04 \pm 0.01 \pm 0.01$	$1.4 \pm 0.5 \pm 0.1 \pm 0.1$
VH	$0.0524^{+0.0031}_{-0.0051}$	$0.067 \pm 0.048^{+0.007}_{-0.004}{}^{+0.011}_{-0.007}$	$1.3 \pm 0.9 \pm 0.1 \pm 0.2$
ttH	$0.0154^{+0.0010}_{-0.0014}$	$0.019^{+0.022}_{-0.013} \pm 0.002 \pm 0.002$	$1.2^{+1.4}_{-0.9} \pm 0.1 \pm 0.1$
Reduced Stage-1.1 production bins, $\lvert y_H \rvert < 2.5$			
ggF-$0j$-p_T^H-Low	0.176 ± 0.022	$0.18 \pm 0.05 \pm 0.02$	$1.00 \pm 0.29 \pm 0.08$
ggF-$0j$-p_T^H-High	0.55 ± 0.05	$0.58 \pm 0.09 \pm 0.05$	$1.06 \pm 0.17 \pm 0.09$
ggF-$1j$-p_T^H-Low	0.172 ± 0.025	$0.13 \pm 0.07 \pm 0.04$	$0.8 \pm 0.4 \pm 0.2$
ggF-$1j$-p_T^H-Med	0.119 ± 0.019	$0.14 \pm 0.04 \pm 0.01$	$1.2 \pm 0.4 \pm 0.1$
ggF-$1j$-p_T^H-High	0.020 ± 0.004	$-0.002^{+0.013}_{-0.009} \pm 0.002$	$-0.1 \pm 0.6 \pm 0.1$
ggF-$2j$	0.125 ± 0.027	$0.06 \pm 0.07 \pm 0.03$	$0.5 \pm 0.5 \pm 0.2$
ggF-p_T^H-High	0.015 ± 0.004	$0.031 \pm 0.020 \pm 0.002$	$2.1 \pm 1.3 \pm 0.2$
VBF-p_T^H-Low	0.0863 ± 0.0030	$0.14 \pm 0.05 \pm 0.01$	$1.7 \pm 0.6 \pm 0.1$
VBF-p_T^H-High	0.00576 ± 0.00022	$0.0003 \pm 0.008 \pm 0.001$	$0.1 \pm 1.5 \pm 0.1$
VH-Had	$0.0359^{+0.0021}_{-0.0035}$	$0.06 \pm 0.06 \pm 0.01$	$1.6^{+1.8}_{-1.4}{}^{+0.3}_{-0.2}$
VH-Lep	$0.0165^{+0.0010}_{-0.0016}$	$0.022^{+0.028}_{-0.017}{}^{+0.002}_{-0.001}$	$1.3^{+1.7}_{-1.0} \pm 0.1$
ttH	$0.0154^{+0.0010}_{-0.0014}$	$0.018^{+0.022}_{-0.013} \pm 0.002$	$1.2^{+1.4}_{-0.8}{}^{+0.2}_{-0.1}$

Differential fiducial cross section $p_T^{4\ell}$

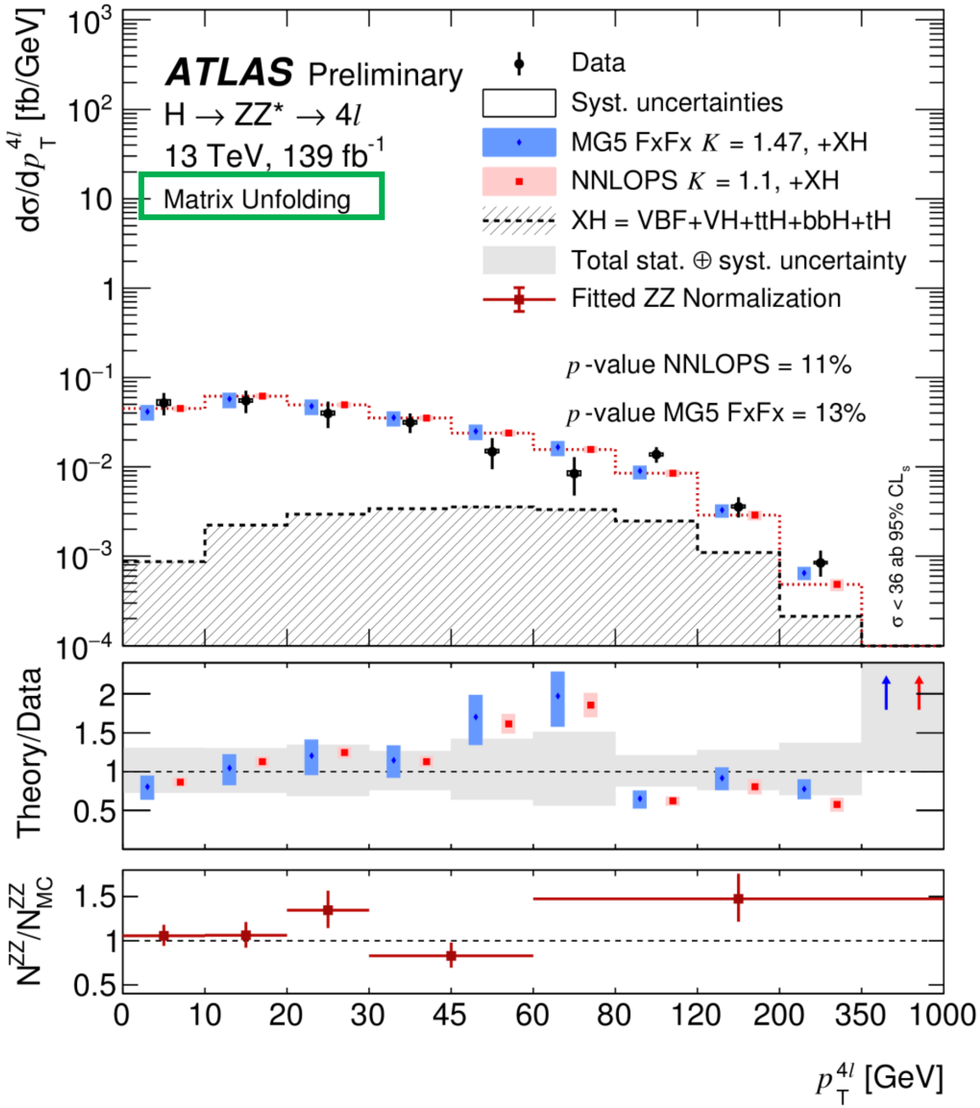

Differential fiducial cross section $p_T^{4\ell}$

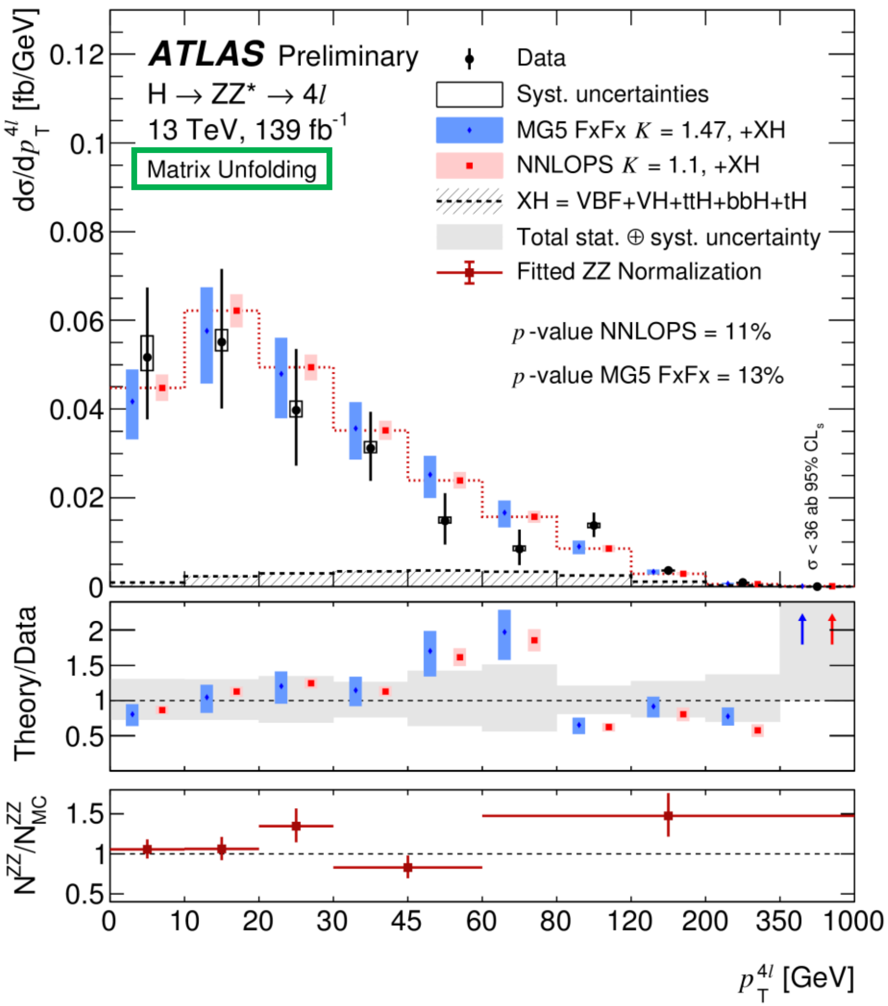

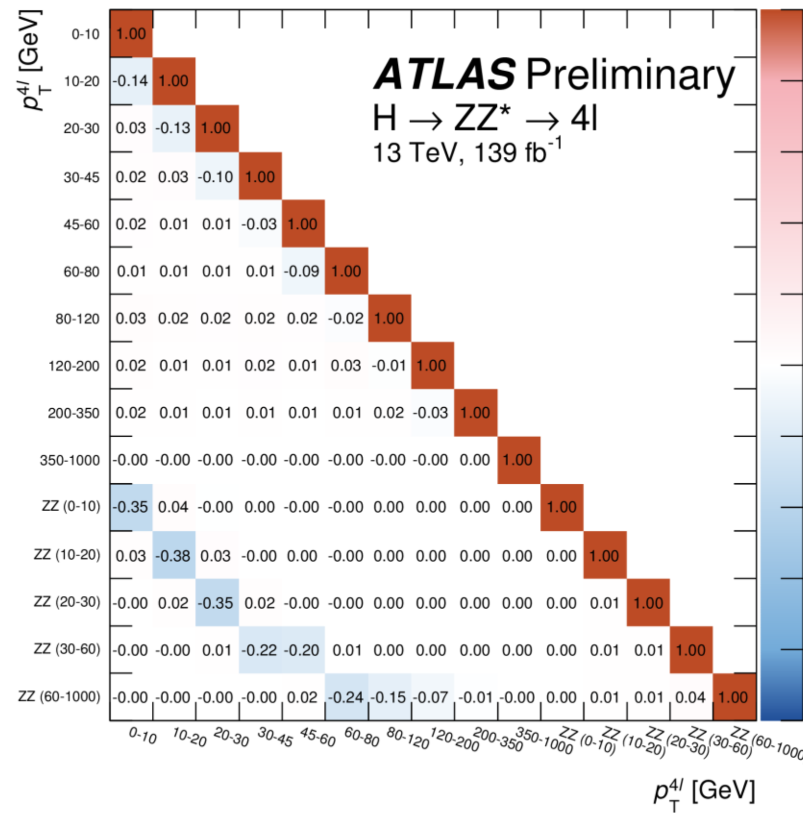

Differential fiducial cross section $p_T^{4\ell}$

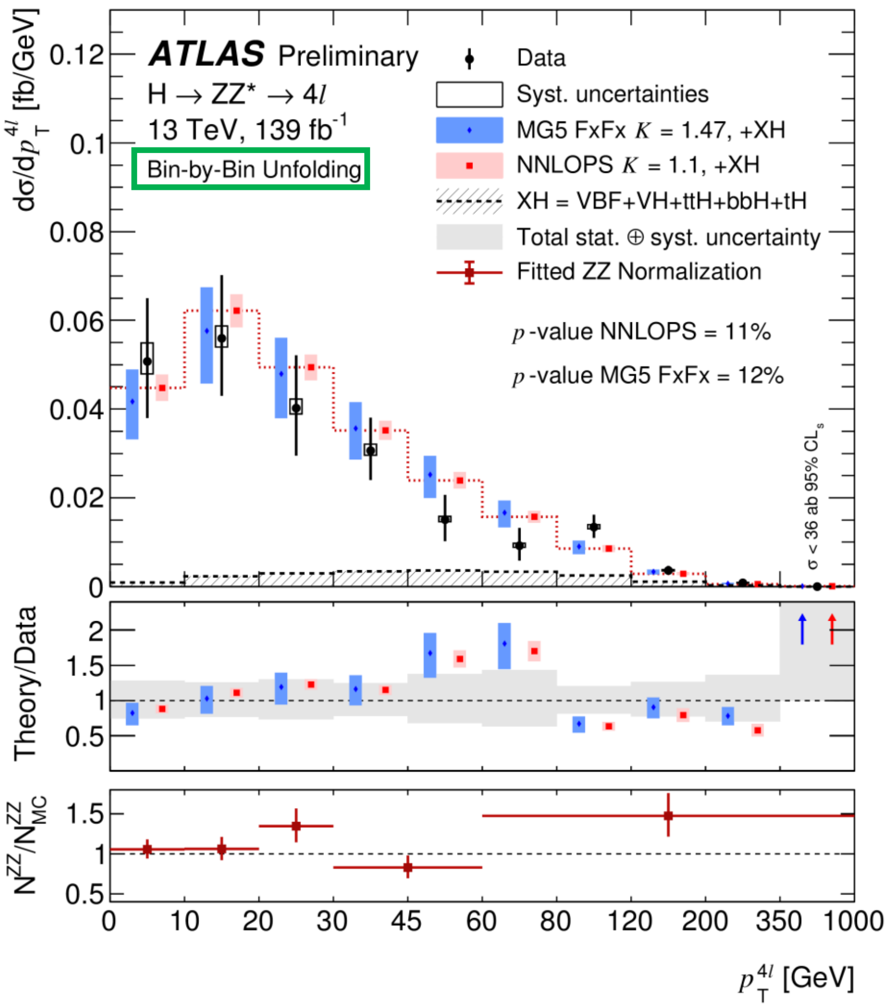

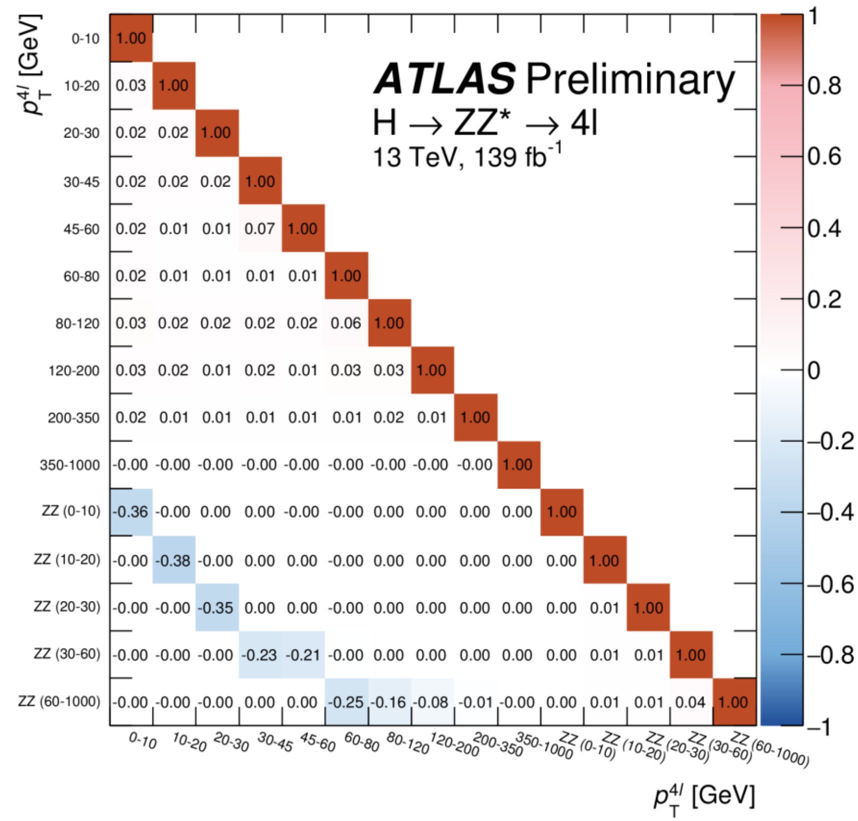

Differential fiducial cross section N_{jets}

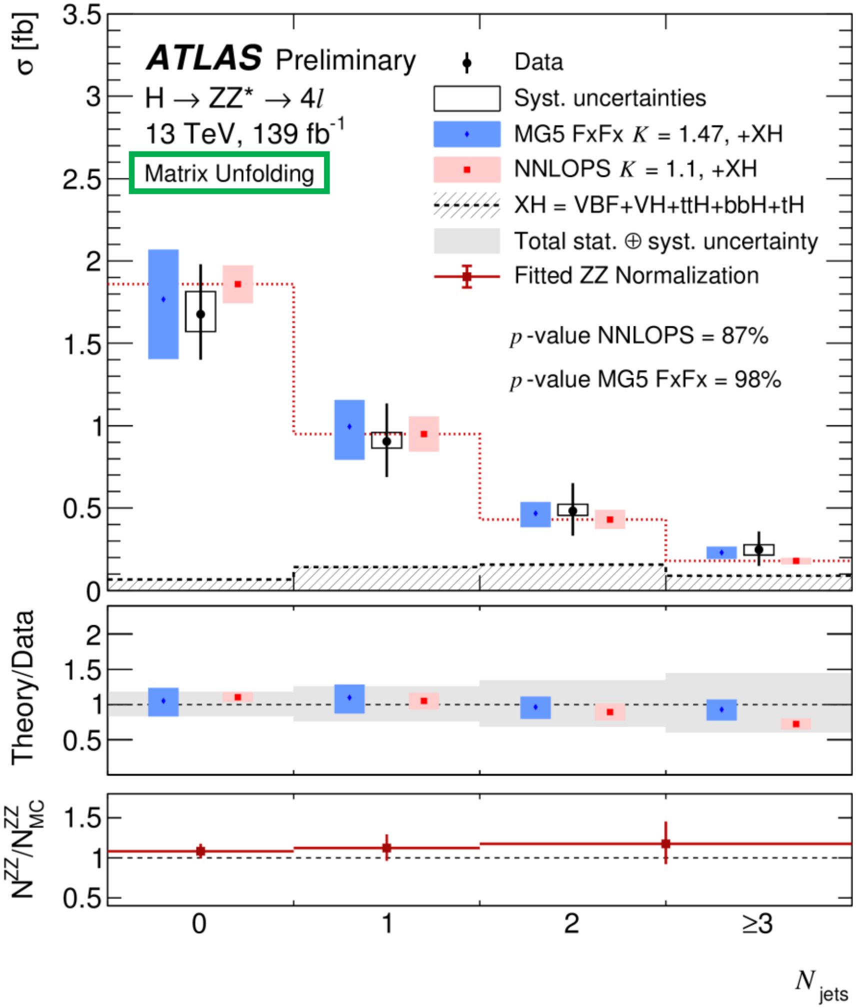

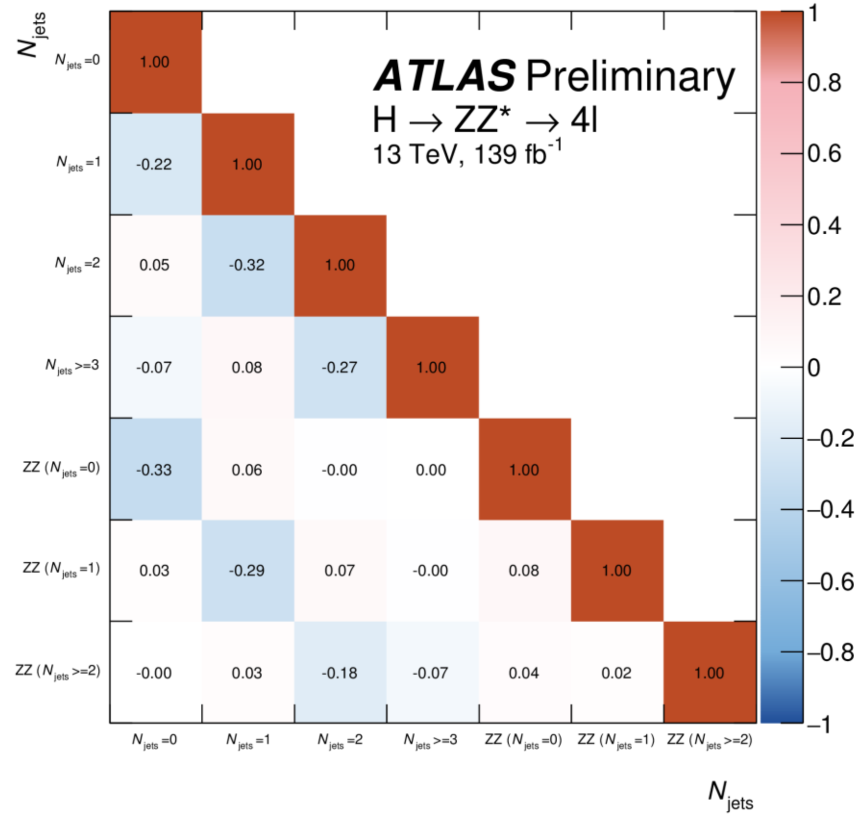

	N_jets=0	N_jets=1	N_jets=2	N_jets>=3	ZZ (N_jets=0)	ZZ (N_jets=1)	ZZ (N_jets>=2)
N_jets=0	1.00						
N_jets=1	-0.22	1.00					
N_jets=2	0.05	-0.32	1.00				
N_jets>=3	-0.07	0.08	-0.27	1.00			
ZZ (N_jets=0)	-0.33	0.06	-0.00	0.00	1.00		
ZZ (N_jets=1)	0.03	-0.29	0.07	-0.00	0.08	1.00	
ZZ (N_jets>=2)	-0.00	0.03	-0.18	-0.07	0.04	0.02	1.00

Differential fiducial cross section N_{jets}

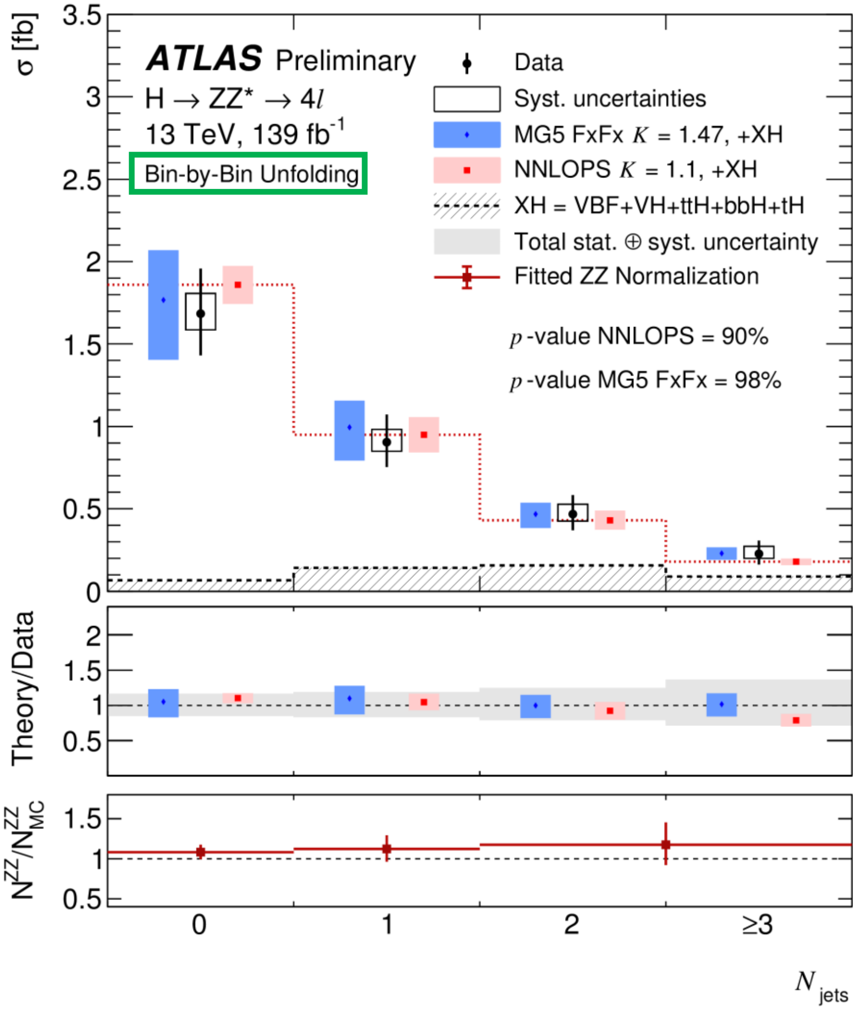

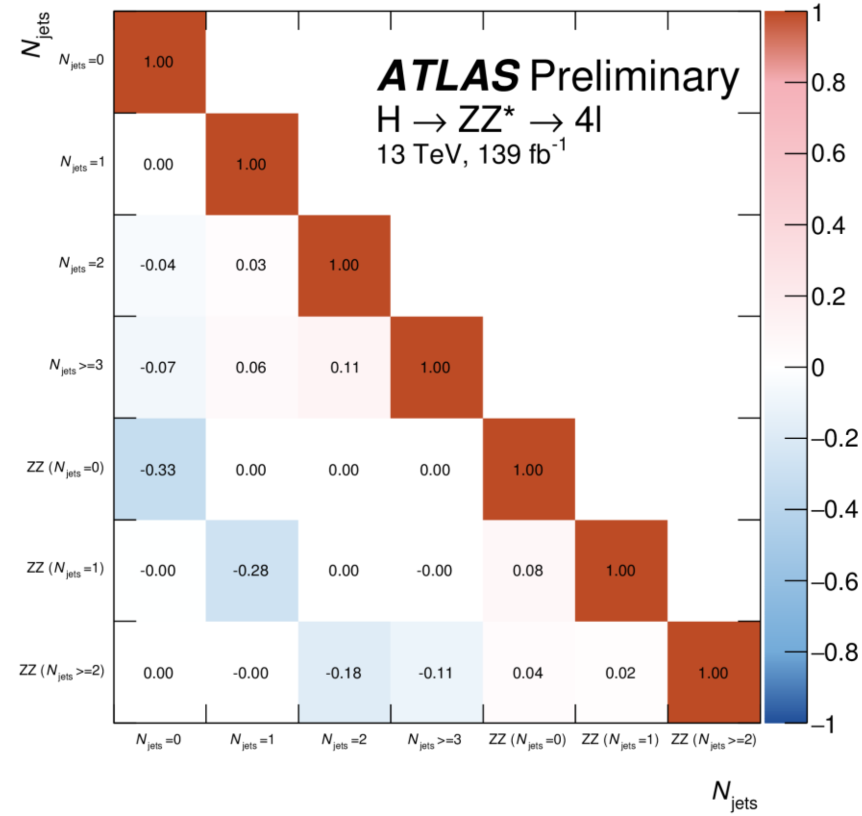

STXS Stage 0

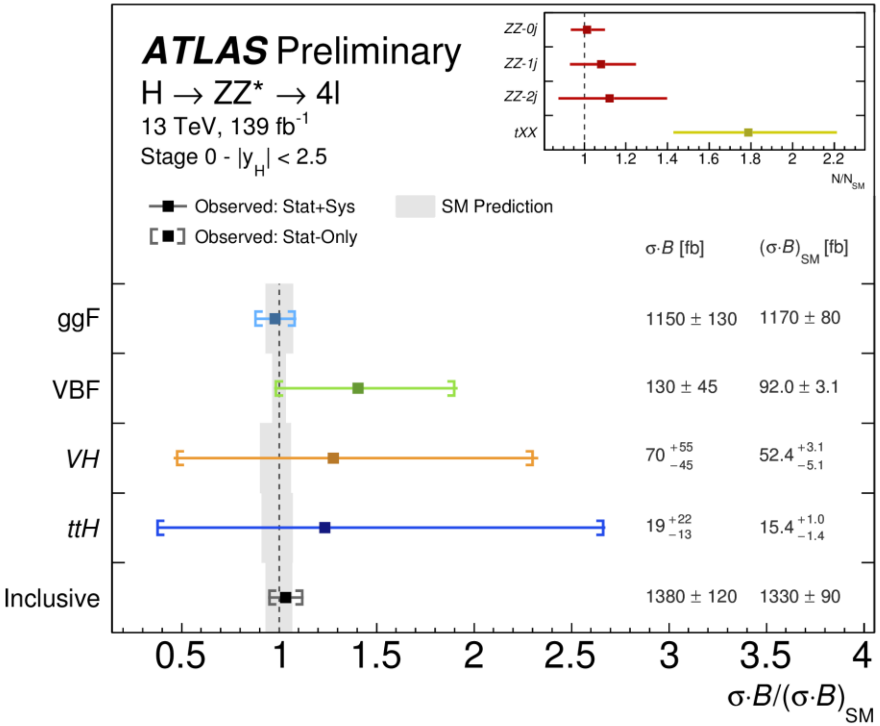
ATLAS Preliminary
H → ZZ* → 4l
13 TeV, 139 fb-1
Stage 0 - |yH| < 2.5
Observed: Stat+Sys
Observed: Stat-Only
SM Prediction
σ·B [fb]
(σ·B)SM [fb]
ggF
VBF
VH
ttH
Inclusive
1150 ± 130
1170 ± 80
130 ± 45
92.0 ± 3.1
70 +55 −45
52.4 +3.1 −5.1
19 +22 −13
15.4 +1.0 −1.4
1380 ± 120
1330 ± 90
ZZ-0j
ZZ-1j
ZZ-2j
tXX
N/NSM
σ·B/(σ·B)SM

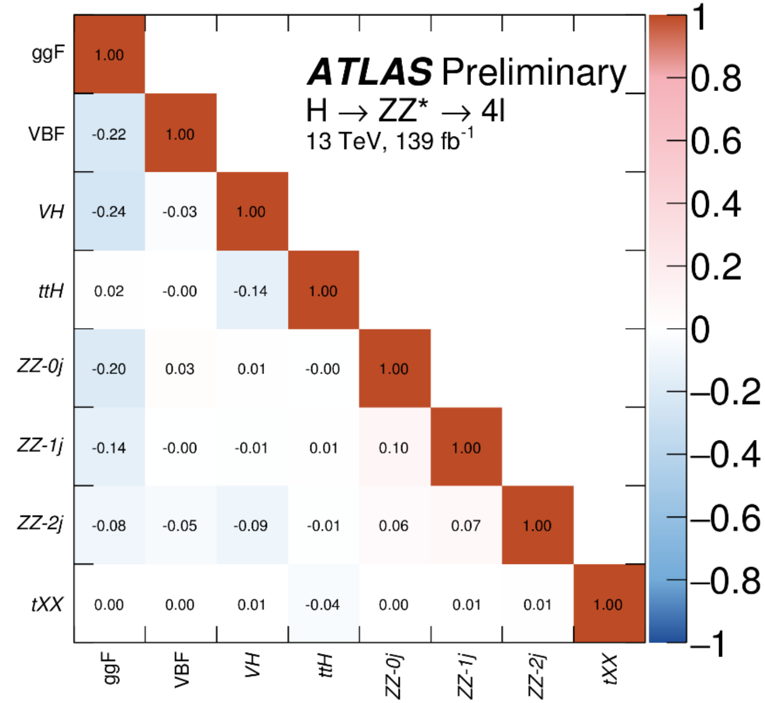
ATLAS Preliminary
H → ZZ* → 4l
13 TeV, 139 fb-1
ggF
VBF
VH
ttH
ZZ-0j
ZZ-1j
ZZ-2j
tXX
1.00
-0.22 1.00
-0.24 -0.03 1.00
0.02 -0.00 -0.14 1.00
-0.20 0.03 0.01 -0.00 1.00
-0.14 -0.00 -0.01 0.01 0.10 1.00
-0.08 -0.05 -0.09 -0.01 0.06 0.07 1.00
0.00 0.00 0.01 -0.04 0.00 0.01 0.01 1.00

STXS reduced Stage 1.1

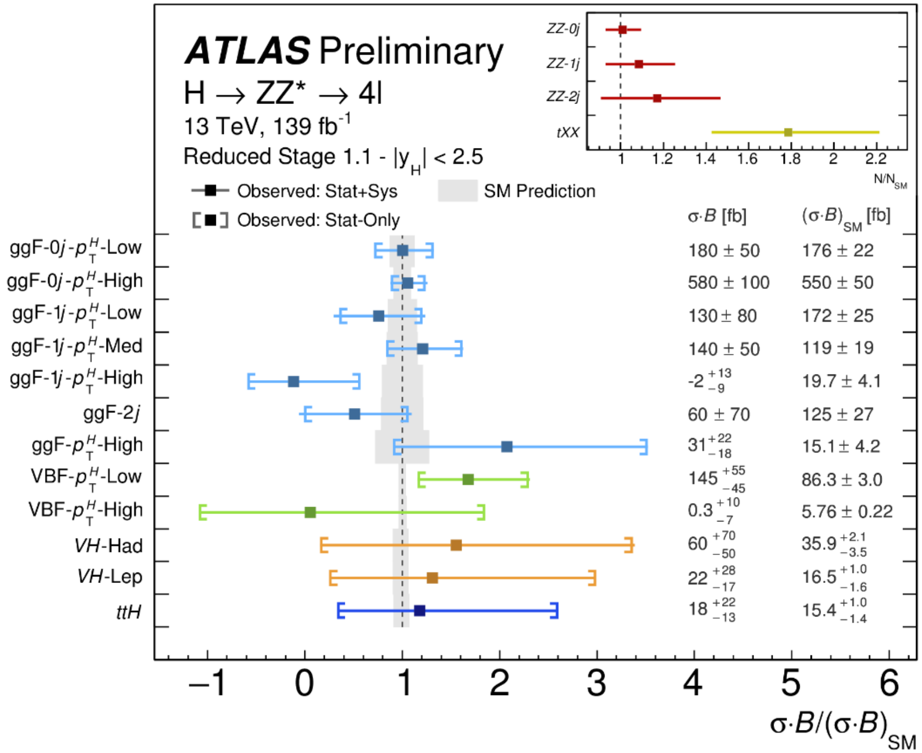

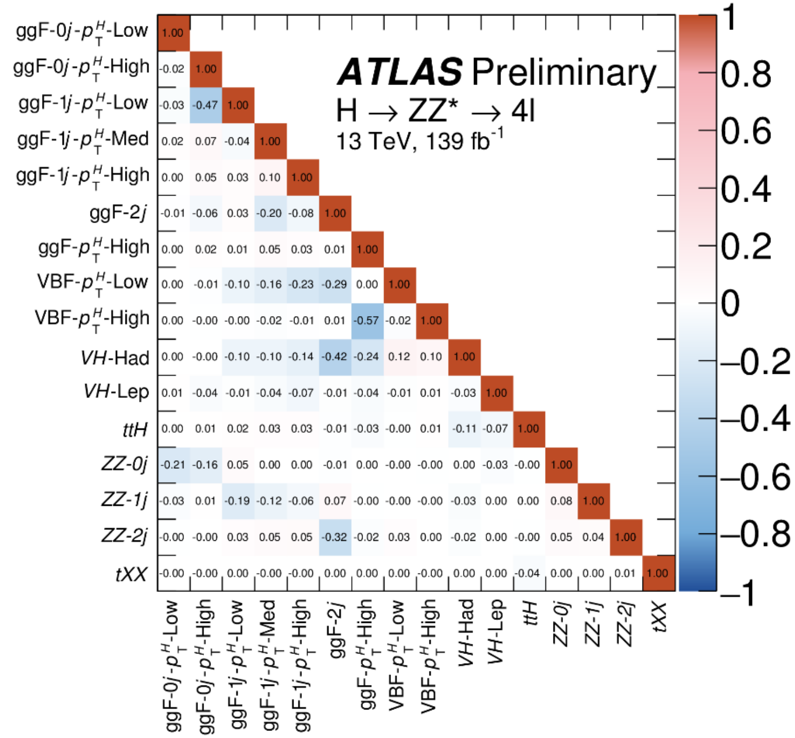

Systematic uncertainties of previous results

Measurement [-0.5ex]	Experimental uncertainties [%] Lum.	e, μ, pile-up	Jets, flavour tagging	Reducible backgr.	Theory uncertainties [%] ZZ^* backgr.	PDF	Signal QCD scale	Parton Shower	Composition
Fiducial cross section									
	2.8	4.3	< 0.1	0.3	1.6	0.6	0.5	0.4	0.1
Per decay channel fiducial cross sections									
4μ	2.8	3.9	< 0.1	0.3	1.6	0.6	0.4	0.6	0.2
$4e$	2.8	9.0	< 0.1	1.0	1.6	0.6	0.8	0.5	0.1
$2\mu 2e$	2.7	8.6	< 0.1	0.9	1.5	0.6	0.7	0.5	0.1
$2e2\mu$	2.8	3.6	< 0.1	0.4	1.8	0.6	0.7	0.5	0.2
Stage-0 production bin cross sections									
ggF	2.9	3.9	1.3	0.7	2.3	0.4	2.1	0.7	-
VBF	1.7	1.5	10.5	0.5	2.3	2.3	9.5	5.1	-
VH	2.0	1.7	7.8	1.8	5.6	2.1	14.9	3.1	-
ttH	2.5	1.9	3.9	1.5	1.9	0.3	8.8	9.6	-

ATLAS-CONF-2018-018 (79.8 fb^{-1})

σ/σ_{SM} vs signal strength

The impact of the theory systematic uncertainties on the signal depends on the kind of measurement that is performed. For signal strength measurements, defined as the measured cross section divided by the SM prediction, each source of theory uncertainty affects both the fiducial acceptance and the predicted SM cross section. For the cross section measurements, only effects on the acceptance need to be considered.

The corresponding likelihood functions are shown in Figure 11. The dominant systematic uncertainty in the cross section measurement is the experimental uncertainty in the lepton efficiency and integrated luminosity measurements. The signal strength measurement is also equally affected by the theoretical uncertainty of the ggF signal yield due to QCD scale variations.

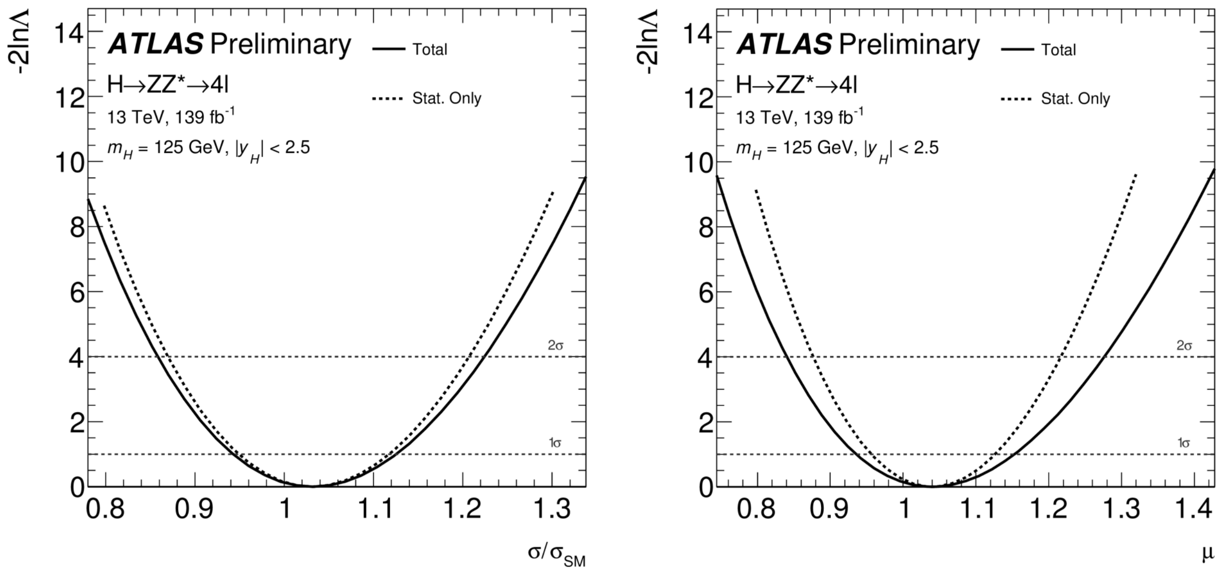

$$(\sigma \cdot \mathcal{B})/(\sigma \cdot \mathcal{B})_{SM} \quad 1.033 \pm 0.08 \pm 0.03 \pm 0.02$$

$$\mu = 1.04^{+0.09}_{-0.08}(\text{stat.})^{+0.04}_{-0.03}(\text{exp.})^{+0.06}_{-0.05}(\text{th.}) = 1.04^{+0.12}_{-0.10}.$$